Deep-Sea Research I 71 (2013) 1–20

Contents lists available at SciVerse ScienceDirect

Deep-Sea Research I

journal homepage: www.elsevier.com/locate/dsri

The role of eddies on particle flux in the Canada Basin of the Arctic Ocean

Mary C. O'Brien [a,*], Humfrey Melling [a], Thomas F. Pedersen [b], Robie W. Macdonald [a]

[a] Department of Fisheries and Oceans, Institute of Ocean Sciences, 9860 W. Saanich Rd., Sidney, BC, Canada V8L 4B2
[b] School of Earth and Ocean Sciences, UVIC PO Box 1700 STN CSC Victoria, BC, Canada V8W 2Y2

ARTICLE INFO

Article history:
Received 25 April 2012
Received in revised form
2 October 2012
Accepted 7 October 2012
Available online 1 November 2012

Keywords:
Arctic
Canada Basin
Particle flux
Sediment transport
Eddies

ABSTRACT

Moorings with sequential sediment traps to study downward sediment flux in the Canada Basin of the Arctic Ocean were maintained in 3350 m of water year-round between September 1990 and July 1994. Sediment was collected nominally at 600-m depth and instruments measuring current, temperature, salinity and pressure were placed at several levels between 45 and 1515 m. Total dry weight particle fluxes were low (4.2, 2.1, and 8.2 g m^{-2} a^{-1}) compared to those found in other world ocean basins. Particle flux varied greatly intra-annually. There were peaks during each summer, with differing seasonal timing and particle composition suggesting a correlation with inter-annual differences in summertime ice clearance. In winter, the particle flux was higher if the ice of the preceding summer was light. Enhanced primary production in summers with wider ice-free seas is a possible explanation, but inconsistent with the high lithogenic (LITH) content of most samples: A significant fraction of the particulate organic carbon (POC) content is refractory carbon. Another possibility is that the south-easterly wind pushing ice to the north-west in summers of reduced ice drives the Mackenzie River plume, laden with lithogenic sediment, behind it and out to the mooring site. There is also another factor in play: Peaks in particle flux frequently coincided with eddies, mesoscale circulation features with strongest current well below the surface. The highest measured flux occurred in the winter of 1994, synchronous with a baroclinic eddy which enveloped the mooring for 60 days while rotating cyclonically and moving slowly north-westward. Particles trapped at this time had high LITH and low POC contents, a relatively high molar ratio of biogenic silica to POC and appreciable chlorophyll *a* and phaeophytin pigments. Subsequent trap intervals coincided with the passage of a deeper anti-cyclonic eddy, also on a north-westward trajectory, which deposited material of different composition. These observations demonstrate that an understanding of the lateral transport of sediment by energetic physical phenomena is critical to the insightful interpretation of the particle flux measured with sediment traps at sites remote from the coast in the southern Canada Basin.

1. Introduction

The emerging picture of particle fluxes in Arctic basins is one where old allochthonous carbon and terrestrial material supplied laterally from the shelves and slopes to the deep basin dominates the transport while autochthonous carbon and vertical transport play minor roles. Although exceptionally large quantities of lithogenic suspended particles are supplied episodically to Arctic continental shelves via river inflows and coastal erosion (Rachold et al., 2004), the biological pump within the Arctic interior ocean is anomalously weak (Honjo et al., 2010; Hwang et al., 2008). Particles supplied from land settle to the shelf bottom but are commonly subject to energetic events (e.g., wind, waves, strong currents, internal waves, ice keel gouging), which facilitate resuspension over shelf and slope and transport to the deep basin. Movement of lithogenic sediment to the deep basin also occurs via ice rafting (Rachold et al., 2004), via the spreading of sediment laden river plumes and via slumping of bottom sediments at the shelf edge and the slope (Grantz et al., 1996).

The large-scale circulation features of the Beaufort Sea, the Gyre and the Shelfbreak Jet (Fig. 1), play important roles in sediment transport. The Beaufort Gyre – a large scale, wind-driven anti-cyclonic circulation – carries sea ice and surface waters around Canada Basin and is a vast reservoir of freshwater from runoff and ice melt (Macdonald et al., 1999; Proshutinsky et al., 2002; Plueddemann et al., 1998). Alternating anti-cyclonic and cyclonic anomalies in the Beaufort Gyre occur on approximately a 5–7 year cycle in response to atmospheric oscillations. These cycles play a significant role in Arctic climate variability by accumulating freshwater during times of anti-cyclonic anomaly and releasing freshwater during times of cyclonic anomaly (Proshutinsky and Johnson, 1997; Proshutinsky et al., 1999,

* Corresponding author. Tel.: +1 250 363 6716.
E-mail addresses: mary.obrien@dfo-mpo.gc.ca, mcob@shaw.ca (M.C. O'Brien).

0967-0637
http://dx.doi.org/10.1016/j.dsr.2012.10.004

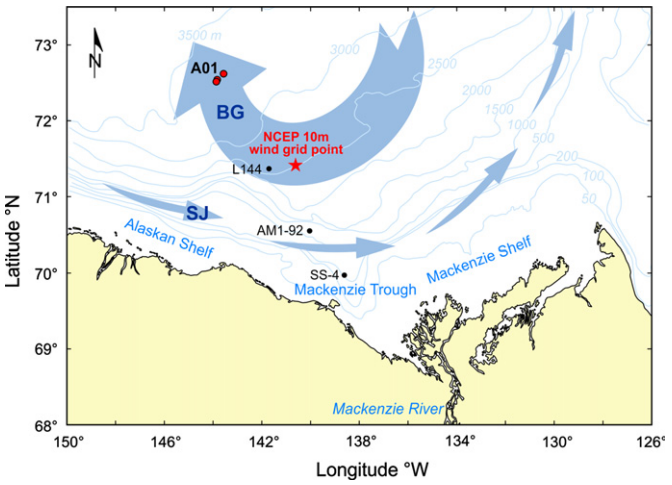

Fig. 1. Location of mooring site A01 (see Table 1) and National Centers for Environmental Prediction (NCEP) grid point (71.426°N 140.625°W). Location of sites from other sequential trap studies (small black dots) are L144 and AM1-92 (O'Brien, 2009) and SS-4 (O'Brien et al., 2006). The large blue arrow labeled BG indicates the dominant direction of the Beaufort Gyre and the smaller blue arrows labeled SJ show the dominant direction of the Shelfbreak Jet. (For interpretation of the references to color in this figure legend, the reader is referred to the web version of this article.)

2002; Morison et al., 2012; Giles et al., 2012). Sediment transport and primary production are closely linked to patterns of freshwater runoff, ice melt, ice drift and wind forcing but we presently have few observational data to inform us about details of those linkages.

At the southern perimeter of the Beaufort Gyre the narrow eastward-flowing boundary current, the Beaufort Shelf-break Jet (Pickart, 2004; Nikolopoulos et al., 2009), is strongly influenced by wind, which modulates its speed and forces reversals in its direction of flow (Kulikov et al., 1998, 2004). Nutrient-rich waters of Pacific and Atlantic origin move eastward in this boundary current. Exchanges of water across the shelf break occur at the surface via Ekman transport and at the seabed via up/downwelling driven by surface stress from wind and ice motion (Macdonald and Wong, 1987; Yang, 2009). Upwelling in the southern Beaufort occurs with easterly winds (Carmack and Kulikov, 1998) and may be sensitive to the position of the ice edge relative to the shelf break (Carmack and Chapman, 2003). Sea valleys that cut across the shelf, such as Mackenzie Trough, are preferred locations for such exchanges (Williams et al., 2006, 2008).

The boundary current and its meanders transport suspended material along and beyond the shelf break (Darby et al., 2009; Ashjian et al., 2005). This current is also a source of eddies that have been observed in the Canada Basin (Pickart, 2004; Mathis et al., 2007). Eddies containing water of locally anomalous temperature–salinity correlation are ubiquitous in the Canada and Amundsen basins. They are most commonly observed within the halocline (Krishfield et al., 2002) but also occur below the halocline to depths greater than 1700 m (Aagaard et al., 2008; references therein). Core waters in eddies may contain elevated concentrations of nutrients, organic carbon and suspended particles (Mathis et al., 2007).

The Mackenzie River supplies the Mackenzie shelf with massive inputs of fresh water and suspended sediment. Despite gravitational settling, Mackenzie sediments travel great distances via wind-driven movement of the river plume. Far less obvious, but perhaps more important than these surface processes, sediment is transported and exported in mid- and bottom-nepheloid layers following re-suspension during storms (O'Brien et al., 2006). Sea-bottom gouging by ice keels as deep as 30 m can return sediment to the water column, where it can be frozen into growing ice and travel thousands of kilometers before its release during the thaw (Eicken et al., 2005).

The conditions for and frequency of sediment resuspension from the shelf and slope are not well understood, nor is the frequency with which resuspension results in transport to deep waters. Without such understanding, the impact on sediment processes by climate change effects – on ice cover, weather, river inflow and its dispersal, coastal erosion, resuspension, the biological pump and suspended sediment transport into Canada Basin – will remain enigmatic. Regrettably there are few data that allow study of these processes, which are essential to the understanding of material budgets in the Arctic, e.g., for carbon, silica, and pollutants.

Here we explore physical processes that transport particles to and within deep Arctic basins using data from three annual sediment trap deployments at the 3300 m isobath in the Canada Basin, September 1990, 1992, and 1993. Data from these traps, collected prior to the recent decline in Arctic summertime sea ice, include total solids, organic carbon, total nitrogen, biogenic silica, and pigments. We interpret these time-series in the context of ice conditions, ocean current, temperature and salinity at the moorings and place them within a broader context of weather, ice and river conditions on the adjacent Beaufort shelf.

2. Data and methods

2.1. Station A01 moorings and supporting data

Records of the downward particle flux, seawater temperature and salinity, ocean current and sea ice in Canada Basin were acquired using sequentially sampling sediment traps and electronic recording instruments on submerged moorings in the early 1990s. These were deployed in 1990, 1992, and 1993 at closely spaced stations A01-90, A01-92, and A01-93 near the 3350 m isobath (Fig. 1, Table 1). Two Baker/Milburn sediment traps (Baker

Table 1
Depths of data records recovered from moorings in the Canada Basin (1990–1994) at sites A01-90, A01-92, and A01-93. Instruments are upward looking sonars (ULS), current meters (RCM4 and RCM5) with temperature (T) and conductivity sensors (C), Seacats measuring temperature and conductivity, and sediment traps as described in Section 2.1.

Site	**A01-90 72.621**	**A01-92 72.542**	**A01-93 72.517**
lat/ lon	**N/143.568 W**	**N/143.830 W**	**N/143.866 W**
Start	September 1990	September 1992	September 1993
End	July 1991 (m)	August 1993 (m)	August 1994 (m)
ULS	72	28	53
RCM4/5	81	46	60
Plus T&C	81	46	60
SeaCat	83	47	62
RCM4/5	~	67	79
Plus T&C	101	67	79
RCM4/5	~	117	93
Plus T&C	~	117	83
RCM4/5	208	167	139
Plus T&C	208	167	139
SeaCat	209	169	140
RCM4/5	331	296	265
Plus T&C	331	296	265
Sediment trap	**615**	**600**	**568**
RCM4/5	633	598	272
Plus T&C	633	598	572
Sediment trap	**1515**		
Seabed	3339	3375	3370

Table 2
Sequential trap schedules and data (composition and fluxes) at each of the three Canada Basin sites (A01-90, A01-92, and A01-93). Abbreviations are: total dry weight (TDW), particulate organic carbon (POC), total nitrogen (TN), biogenic silica (BIOSI), chlorophyll *a* (CHLA), and phaeophytins (PHAEO).

Sequence #	Start date	Interval (days)	Collection area (m^2)	TDW flux ($mg\ m^{-2}\ d^{-1}$)	% POC	POC flux ($mg\ m^{-2}\ d^{-1}$))	% TN	TN flux ($mg\ m^{-2}\ d^{-1}$))	C:N molar ratio	% BIOSI	BIOSI flux ($mg\ m^{-2}\ d^{-1}$))	CHLA flux ($\mu g\ m^{-2}\ d^{-1}$)	PHAEO flux ($\mu g\ m^{-2}\ d^{-1}$)
Station A01-90 (615 m) < 500 μm fraction (72.621°N/143.568°W; water depth of 3339 m)													
1	03/09/1990 20:40	33.38	0.032	2.42	7.38	0.18	0.72	0.02	11.95				
2	07/10/1990 5:41	32	0.032	3.39	6.30	0.21	0.86	0.03	8.54				
3	08/11/1990 5:41	32	0.032	1.97	8.16	0.16	1.10	0.02	8.65				
4	10/12/1990 5:41	32	0.032	3.96	6.32	0.25	0.69	0.03	10.68				
5	11/01/1991 5:41	32	0.032	6.28	4.73	0.30	0.49	0.03	11.26				
6	12/02/1991 5:41	32	0.032	1.82	7.95	0.14	1.29	0.02	7.19				
7	16/03/1991 5:41	32	0.032	1.30	10.63	0.14	1.56	0.02	7.95				
8	17/04/1991 5:41	32	0.032	2.97	9.84	0.29	1.66	0.05	6.91				
9	19/05/1991 5:41	32	0.032	5.13	7.49	0.38	1.22	0.06	7.16				
10	20/06/1991 5:41	32	0.032	59.64	6.17	3.68	1.04	0.62	6.91	2.70	1.610	0.09	2.00
Station A01-90 (1515 m) < 500 μm fraction (72.621°N/143.568°W; water depth of 3339 m)													
1	03/09/1990 18:40	33.45	0.032	2.58	6.59	0.17	0.49	0.01	15.68				
2	07/10/1990 5:32	32	0.032	1.55	8.23	0.13	1.03	0.02	9.32				
3	08/11/1990 5:32	32	0.032	4.25	5.68	0.24	0.68	0.03	9.74				
4	10/12/1990 5:32	32	0.032	30.92	4.46	1.38	0.60	0.18	8.74	3.20	0.990	0.07	1.60
5	11/01/1991 5:32	32	0.032	42.01	3.71	1.56	0.45	0.19	9.60	3.17	1.330	0.00	0.00
6	12/02/1991 5:32	32	0.032	26.15	4.04	1.06	0.52	0.14	9.15	3.57	0.930	0.00	0.00
Station A01-92 (600 m) < 500 μm fraction (72.542°N/143.830°W; water depth of 3375 m)													
1	25/09/1992 0:00	27	0.509	1.69	13.49	0.23	2.11	0.04	7.47	5.93	0.100	0.02	1.77
2	22/10/1992 0:00	27	0.509	1.27	12.41	0.16	1.96	0.02	7.39	5.65	0.072	0.01	0.90
3	18/11/1992 0:00	27	0.509	6.51	7.40	0.48	1.17	0.08	7.37	7.02	0.457	−0.16	3.63
4	15/12/1992 0:00	27	0.509	1.46	9.37	0.14	1.43	0.02	7.62	5.45	0.080	0.00	0.54
5	11/01/1993 0:00	27	0.509	0.72	39.14	0.28	6.61	0.05	6.90	0.58	0.004	0.00	0.15
6	07/02/1993 0:00	27	0.509	0.58	27.97	0.16	5.35	0.03	6.10	1.94	0.011	0.00	0.14
7	06/03/1993 0:00	27	0.509	0.58	16.19	0.09	2.87	0.02	6.57	4.73	0.028	0.01	0.13
8	02/04/1993 0:00	27	0.509	0.53	13.69	0.07	2.55	0.01	6.25	3.53	0.019	0.00	0.11

Table 2 (*continued*)

Sequence #	Start date	Interval (days)	Collection area (m^2)	TDW flux ($mg\ m^{-2}\ d^{-1}$)	% POC	POC flux ($mg\ m^{-2}\ d^{-1}$))	% TN	TN flux ($mg\ m^{-2}\ d^{-1}$))	C:N molar ratio	% BIOSI	BIOSI flux ($mg\ m^{-2}\ d^{-1}$))	CHLA flux ($\mu g\ m^{-2}\ d^{-1}$)	PHAEO flux ($\mu g\ m^{-2}\ d^{-1}$)
9	29/04/1993 0:00	27	0.509	0.36	16.74	0.06	3.27	0.01	5.98	2.26	0.008	0.01	0.13
10	26/05/1993 0:00	27	0.509	2.59	10.43	0.27	1.25	0.03	9.72	4.00	0.103	0.18	1.82
11	22/06/1993 0:00	27	0.509	9.88	9.99	0.99	0.95	0.09	12.21	8.49	0.839	0.38	5.38
12	19/07/1993 0:00	27	0.509	43.51	7.70	3.35	0.77	0.33	11.67	5.27	2.291	1.82	59.69
13	15/08/1993 0:00	15	0.509	6.22	5.85	0.36	0.78	0.05	8.73	4.76	0.296	0.08	3.78
Station A01-93 (568 m) < 500 μm fraction (72.517°N/143.866°W; water depth of 3370 m)													
1	03/09/1993 0:00	30	0.509	35.32	7.01	2.48	1.00	0.35	8.21	5.70	2.015	0.27	11.43
2	03/10/1993 0:00	30	0.509	14.65	6.33	0.93	0.85	0.13	8.64	5.44	0.796	0.07	6.83
3	02/11/1993 0:00	30	0.509	21.56	5.93	1.28	0.86	0.18	8.07	7.51	1.619	−0.12	5.47
4	02/12/1993 0:00	30	0.509	16.24	6.61	1.07	0.90	0.15	8.54	9.80	1.591	0.19	6.92
5	01/01/1994 0:00	30	0.509	44.03	4.97	2.19	0.62	0.27	9.29	8.26	3.636	0.35	14.98
6	31/01/1994 0:00	30	0.509	65.11	4.66	3.03	0.69	0.45	7.92	6.03	3.929	0.44	13.14
7	02/03/1994 0:00	30	0.509	7.02	20.05	1.41	3.85	0.27	6.07	2.28	0.160	0.03	0.47
8	01/04/1994 0:00	30	0.509	8.75	16.03	1.40	2.73	0.24	6.86	3.17	0.277	0.01	0.55
9	01/05/1994 0:00	30	0.509	9.24	29.23	2.70	5.39	0.50	6.32	1.15	0.106	0.01	0.22
10	31/05/1994 0:00	30	0.509	18.91	29.44	5.57	3.69	0.70	9.31	4.17	0.789	0.04	1.32
11	30/06/1994 0:00	30	0.509	1.56	10.45	0.16	1.83	0.03	6.65	3.56	0.056	0.05	1.27
12	30/07/1994 0:00	30	0.509	28.69	4.41	1.26	0.59	0.17	8.65	4.42	1.269	0.02	5.29

and Milburn, 1983) were used at A01-90 and samples were recovered for nine full 32-day intervals at 615 m and six at 1515 m. Single Parflux Mark 6–13 sediment traps were used at A01-92 and at A01-93. Thirteen samples each representing 27 days were recovered from A01-92 and twelve samples each representing 30 days from A01-93. The Baker/Milburn sediment traps had a collection area of 0.032 m^2 and the Parflux Mark 6–13, a much larger 0.509 m^2 aperture (Honjo and Doherty, 1988); both trap types were fitted with baffles. Electronically recording instruments on the moorings included Aanderaa types RCM4 and RCM5 current meters with additional sensors for seawater temperature, conductivity and in some cases pressure, Sea Bird SeaCats for measuring temperature, conductivity and in some cases pressure and APL-UW's upward looking sonar for measuring sea-ice presence and draft. The depths of instruments from which useful records were obtained are listed with other mooring details in Table 1. The sediment traps' schedules and data are summarized in Table 2.

Mackenzie River discharge was obtained from the Water Survey of Canada (HYDAT CD-ROM). Wind velocity at a 10 m elevation (numerically hind-cast at 6 h intervals) was obtained from the National Centers for Environmental Prediction (NCEP) for the grid point 71.426°N 140.625°W. Ice conditions were summarized from charts prepared by the Canadian Ice Service (http://www.ec.gc.ca/glaces-ice/).

2.2. Analytical methods

In preparation for deployment, the traps' cups were acid cleaned and filled with a preservative solution (0.2 μm filtered seawater from the intended trap depth, mercuric chloride (1–2 g L^{-1}) as a preservative, and sodium chloride (8–10 g L^{-1}) to create a higher density. On recovery, samples were kept cool in the dark to allow the trapped particles to settle and to prevent alterations to pigment contents. Samples were passed through an acid cleaned 500 μm NITEX sieve and the <500 μm fractions were split using a McLane rotary splitter. Sub-samples were prepared for analysis of total dry weight (TDW) and particulate organic carbon (POC), total nitrogen (TN), biogenic silica (BIOSI), chlorophyll *a* (CHLA), and phaeophytins (PHAEO) contents. Throughout the analysis, duplicates were run to assess analytical precision.

Sub-samples for determining TDW and BIOSI were filtered onto 0.45 μm Nuclepore filters, rinsed with DMQ, dried at 50 °C, cooled in desiccators, and weighed to constant weight. The sum of the weights on these filters divided by the fraction of the total sample represented was used to calculate the total weight in each cup. The TDW flux (mg m^{-2} d^{-1}) for each interval was calculated by dividing the total weight in each cup by the collection area of the trap and the collection period in days. The calculation of annual average fluxes was complicated by missing intervals at the end of each deployment: 43.6, 27, and 5 days for the A01-90, A01-92, and A01-93 deployments, respectively. In calculating annual averages, values for the missing intervals were estimated as the average from the first and last samples of the deployment.

BIOSI was determined by extracting amorphous silica from the sample with 2 M Na_2CO_3 and then measuring the dissolved silicon concentration in the extract by molybdate-blue spectrophotometry based on the method by Mortlock and Froelich (1989). The pooled standard deviation based on the replicates was $Sp=1.95$ μg Si/mg ($n=9$) for the range 6.3 to 306.9 μg Si/mg. No correction was applied for potential leaching of silica from aluminosilicates or for dissolution of radiolarians. However, Mortlock and Froelich (1989) demonstrated that systematic errors due to these effects are small compared to the range of opal contents encountered. Given the high clay content of sediments on the Beaufort shelves and in Mackenzie River suspended particulates, it is recommended that future analysis on samples from this area be done by methods that account for any interference by lithogenic silica (Ragueneau and Treguer, 1994; Conley, 1998; Ragueneau et al., 2005). Analysis of BIOSI was not possible for the very small samples at site A01-90 (in the TDW flux range of 1.3 to 6.3 mg m^{-2} d^{-1}) and consequently, percent lithogenic (% LITH) and percent biogenic (% BIOG) have not been estimated for those samples. For both A01-92 and A01-93, there was a complete set of BIOSI data.

Samples for the analysis of POC and TN were filtered onto quartz filters for the samples from stations A01-92, and A01-93, and onto silver filters (25 mm) for the samples from station A01-90. The inorganic carbon was removed by the addition of 100 to 300 μL of 0.5 N HCl, which was left on the sample for 1/2 h and then dried at 50 °C. The samples plus filters were tamped into pre-combusted nickel sleeves and analyzed on a Leeman CE440 Elemental Analyzer. The instrument was standardized frequently with acetanilide, instrument blanks were run throughout the analysis to ensure instrument stability, and filter blanks were run to correct for filter contributions. No corrections were made for dissolution of POC and TN in the supernatant during the period of deployment and during sample handling so the results reported for POC and TN must be considered as minimum values. Fifty-six samples were run in duplicate and the pooled standard deviation (*Sp*) was calculated for the POC analysis ($Sp=0.25\%$) and the TN analysis ($Sp=0.045\%$). Inorganic carbon was not measured due to the variable presence of carbonates in the resuspended sediments in this area—8 to 27% in Mackenzie Shelf surface sediments (Pelletier, 1984). Contribution by planktonic marine carbonate shells such as foraminifera and coccolithophorids is assumed to be insignificant as few were observed microscopically.

CHLA and PHAEO were analyzed using a Turner Design fluorometer calibrated with pure chlorophyll *a* following the method outlined in Parsons et al. (1984). Care was taken to keep the samples cold and in the dark before analysis.

2.3. Definition of biogenic and lithogenic fractions

Percent POC was converted to particulate organic matter (POM) via a conversion factor of 1.87 based on a mean algal elemental composition of $C_{106}H_{175}O_{42}N_{16}P$ as proposed by Anderson (1995). Note that it is expected that some (maybe most for some samples) of the organic carbon measured may be old refractory carbon from a terrestrial source; therefore, the calculated POM must be considered an upper limit because the conversion factor for refractory organic carbon is lower (O'Brien, 2009) than for algal elemental composition. The POM flux was determined from the % POM of the TDW flux. Finally, % BIOSI was converted to % OPAL by multiplying by 2.4 to account for the average water content of diatomaceous silica (Mortlock and Froelich, 1989). The OPAL flux was determined from the % OPAL of the TDW flux.

The biogenic (BIOG) fractions of the trap samples were estimated as the sum of the POM and OPAL in the sample and the lithogenic (LITH) fraction was estimated as the total sample minus the biogenic fraction. Many of the samples were too small to analyze for aluminum, so that it was not possible to estimate the fraction of POM contributed by old refractory carbon from terrestrial (rather than autochthonous carbon) sources, as described in O'Brien et al. (2006).

3. Results

3.1. Sediment flux and composition

The following discussion of sediment flux at A01 and its composition is based on the data in Table 2 and the summary in Fig. 2.

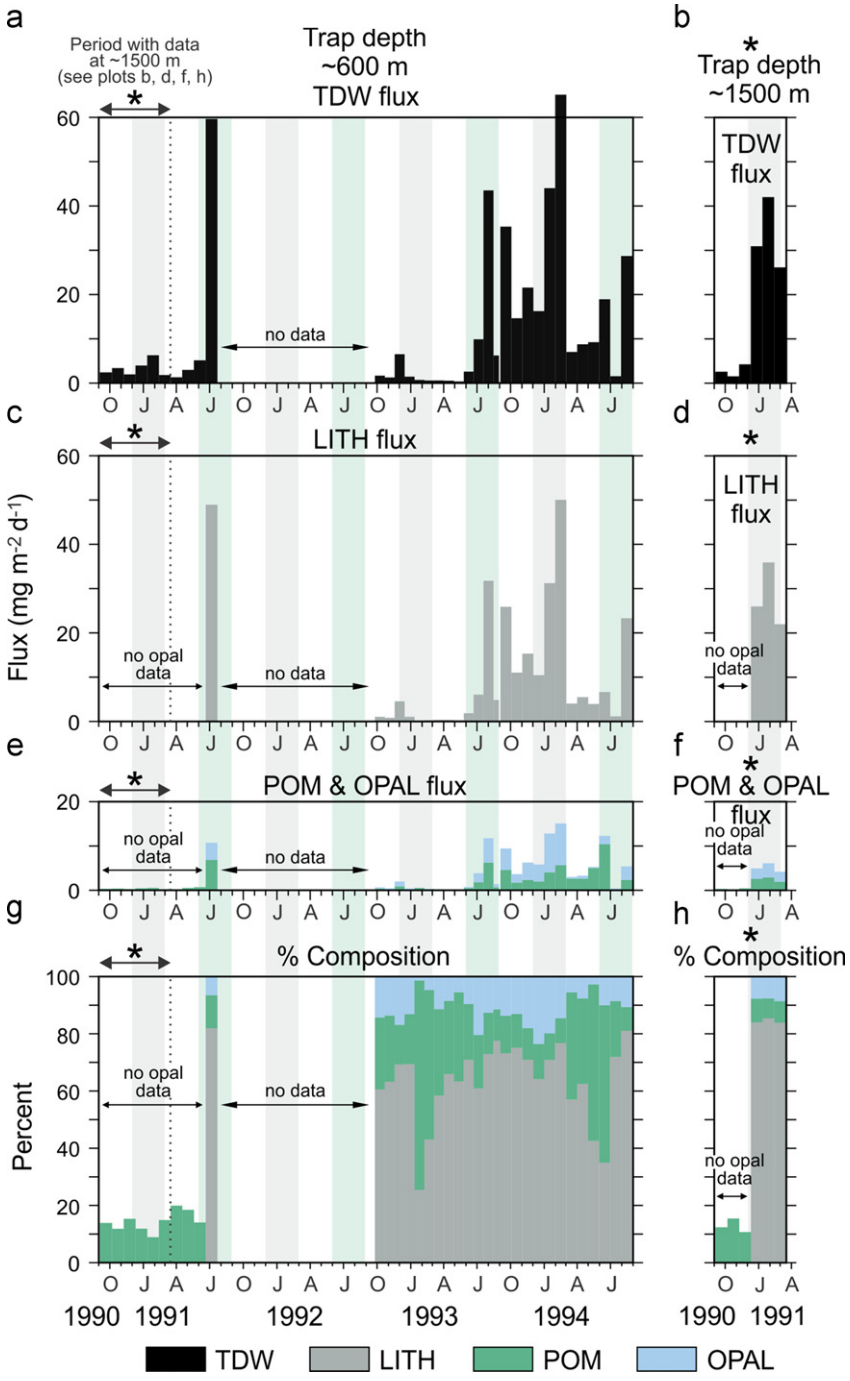

Fig. 2. The plots on the left are for the three sediment traps deployed at ~600 m (A01-90, A01-92, and A01-93) and the smaller plots on the right are for the short deployment at 1515 m at A01-90. The time period marked by an asterisk (*) indicates where there is trap data for both ~600 m and 1515 m (September 3, 1990 to March 16, 1991). Parameters plotted for the trapped material are as follows: total dry weight (TDW) flux (plots a and b), lithogenic (LITH) flux (plots c and d), biogenic flux (sum of particulate organic matter (POM) flux and opaline silica (OPAL) flux; plots e and f) and percent composition (plots g and h) of LITH, POM and OPAL. In some cases, small sample sizes precluded a complete set of analysis; no OPAL data for some samples (1990–1991) meant that terrigenous fluxes could not be calculated. Winter (Dec–Feb) is indicated by light grey bars running between the plots and summer (Jun–Aug) by light green bars. (For interpretation of the references to color in this figure legend, the reader is referred to the web version of this article.)

The median value TDW flux was 5.13 mg m^{-2} d^{-1}, but month-to-month values ranged widely, between 0.4 and 65.1 mg m^{-2} d^{-1}. The composition was generally lithogenic (median 69.4%) but also variable (LITH 25–85%). Median values for POM were 14.4% (range 6.9–73.2%), for OPAL 10.6% (range 1.4–23.5%) and for BIOG 31% (range 15–75%). Note that there was one unusually high % POM (73.2%) value which coincided with a very low TDW flux; there were no obvious analytical problems but there is the possibility of higher analytical error associated with the analysis of very small samples.

The three estimates of average annual TDW flux near 600 m depth at A01 (4.2, 2.1, 8.2 g m^{-2} a^{-1}) varied by a factor of four, but all values are low by global standards. At 1515 m (1990–1991 only), we can estimate only a lower bound for the annual TDW flux, 4.4 g m^{-2} a^{-1}; the annual record was missing 171.5 days in the spring, summer and fall of 1991.

There was no obvious repeated seasonal pattern in fluxes. Lithogenic and biogenic fluxes were low during the 1990 and 1992 fall-winter periods, but much higher during the 1993 fall-winter period, by up to ten times for LITH and seven times for BIOG (Fig. 2).

Despite the 43.6 and 27-day intervals without data coverage in the late summers of 1991 and 1993, there were peaks in LITH and BIOG fluxes during every spring and summer, albeit with different timing, composition and magnitude. The highest LITH fluxes occurred in summer 1991 and winter 1994. Spring–summer peaks in BIOG flux contained little pigment in 1991 and 1994, but that in 1993 was relatively rich in both CHLA and PHAEO; these characteristics are indicative of exported primary production during that year.

Peaks in mid-winter had high LITH and low POC content. A small (6.3 mg m^{-2} d^{-1}) mid-winter peak in TDW flux at 615 m during 1990–1991 coincided with a much larger (42.0 mg m^{-2} d^{-1}) peak at 1515 m. The peaks at both depths were characterized by lowered % POC and elevated % LITH. There was only one TDW peak (6.5 mg m^{-2} d^{-1}) late in the fall of 1992–1993; it coincided with the lowest % POC value (7%) of that period (Fig. 3a). The fall-winter period of 1993–1994 was markedly different: peaks in TDW flux were much higher (maximum of 65.1 mg m^{-2} d^{-1}) and the % POC was lower (4.7–7.0%). However, the lowest % POC again coincided with the highest % LITH (50 mg m^{-2} d^{-1}), in February 1994. At this time, however, the BIOG flux also reached its highest value (15 mg m^{-2} d^{-1}) in association with low but significant fluxes of CHLA and PHAEO (Fig. 3b).

The ups and downs in BIOG and LITH fluxes were generally congruent. BIOG content was typically less than half, with two exceptions (Fig. 3a). The first occurred in January–February 1993 (trap intervals 5–6 of A01-92) when both TDW and pigment fluxes were low. The second (57–65% BIOG) occurred in May–June 1994 (trap intervals 9–10 of A01-93) and was comprised primarily of POM with relatively little OPAL (i.e., low BIOSI:POC ratio) and low pigment fluxes.

There was an abrupt change in the composition of trapped material following the peak in February 1994 (trap intervals 5–6 of A01-93). The peak in February was highly lithogenic, with a relatively high BIOSI:POC ratio, significant pigment flux and low % POC. During March–June 1994 (trap intervals 7–10 of A01-93) trapped sediment had generally higher BIOG contents and low OPAL, BIOSI:POC ratio and pigment fluxes.

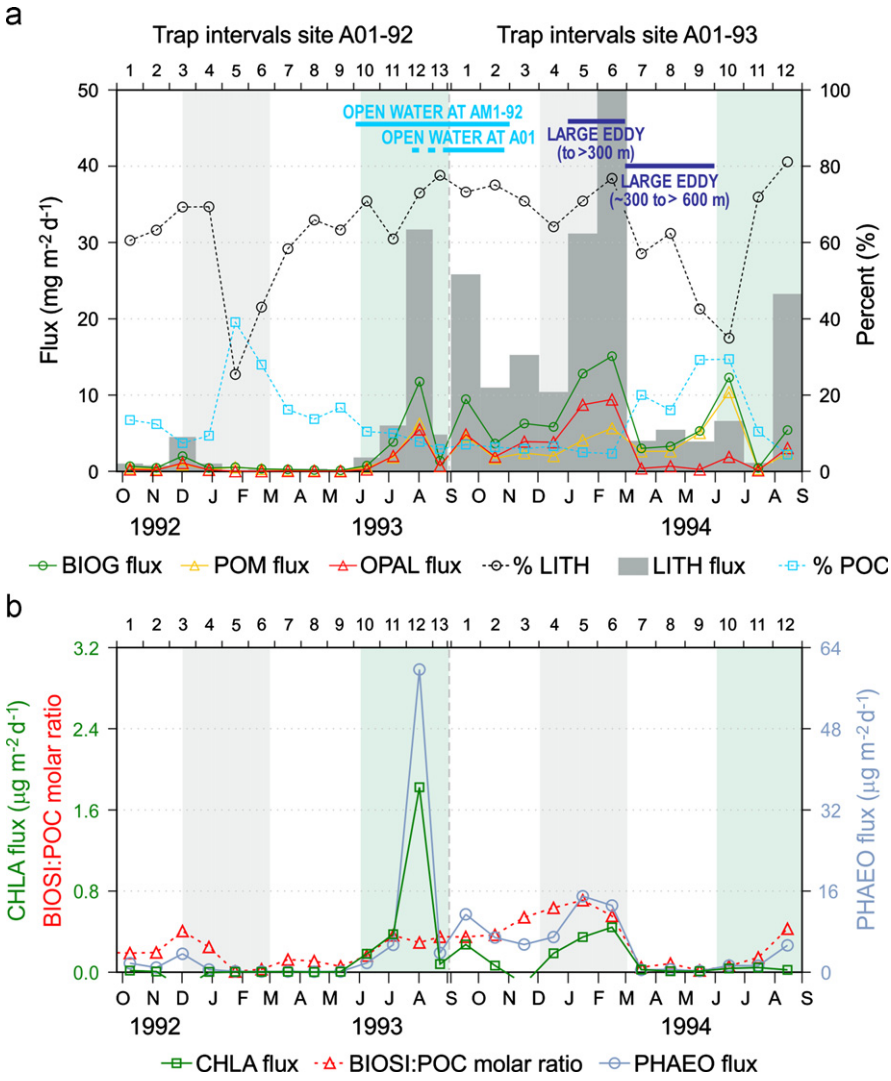

Fig. 3. Fluxes and compositions of trapped material at sites A01-92 and A01-93. (a) Plots of lithogenic (LITH) flux (grey bar plot), % LITH, OPAL flux, particulate organic matter (POM) flux, percent particulate organic carbon (POC) and biogenic (BIOG flux). Note that the fluxes are represented by a symbol and a solid line and referenced to the left *y*-axis. Percentages are represented by a symbol and a dotted line and referenced to the right *y*-axis. Also shown are periods of open water at sites AM1-92 and A01 (see Fig. 1) in 1993 and periods coinciding with two large eddies (at the depths indicated) during the A01-93 deployment. (b) Plots of chlorophyll *a* (CHLA) flux, phaeophytin (PHAEO) flux, and molar ratios of biogenic silica to organic carbon (BIOSI:POC). As in Fig. 2, winter (Dec–Feb) is indicated by light-grey bars running between the plots and summer (Jun–Aug) by light-green bars. (For interpretation of the references to color in this figure legend, the reader is referred to the web version of this article.)

3.2. Ocean variability

Observations of ocean conditions at the A01 moorings during the period of study are summarized in Figs. 4–6. The variables presented in this three-part figure are the daily mean draft of sea ice (panel a), the pressure measured at one level of the mooring (panel b) revealing occasional pull-down of the instruments by strong current, anomalies in potential density (gamma-0) at constant depth (panel c) and speed of current at various instrument depths (panel d). The labeled tick marks on the time axis mark the transitions from one cup of the sediment trap to the next.

Ice was present at A01 at almost all times during the 1990–1991 and 1992–1993 deployments. There were only brief openings, in the fall of 1990 and again in the late summer of 1993. The latter opening continued into the 1993–1994 deployment, with nearly 60 days of ice-free conditions over the mooring at A01 before freeze-up in late October 1993.

The speed of current at all depths was less than 10 cm s^{-1} for at least 79% of the time during the three years of measurement. The occurrences of values less than 5 and 2 cm s^{-1} were greater at deeper levels. However, there were intervals of relatively strong current below 250 m depth throughout the record and notably during 1993–1994. Events with current strong enough (>15 cm s^{-1}) to pull down the moorings occurred during all three deployments at A01 and it is very likely that this led to under trapping of settling particles in the traps (Buesseler et al., 2007 and references therein). In many instances the distinctive depth–time varying signatures in current speed, direction and vertical displacement of isopycnal lines, implicate the passage of baroclinic eddies across the mooring site as the cause of the events.

Baroclinic eddies are maintained by internal density gradients in the ocean that result from slope in isopycnal surfaces. Eddies that rotate anti-cyclonically are characterized by depressions in the isopycnal surfaces of the lower halocline; cyclonic eddies are linked to doming deep isopycnals. The near-surface circulation of eddies under sea ice is typically slowed by friction against the ice, so that there is a sub-surface maximum in the speed of circulation. The slowing is reflected in a reversed isopycnal anomaly

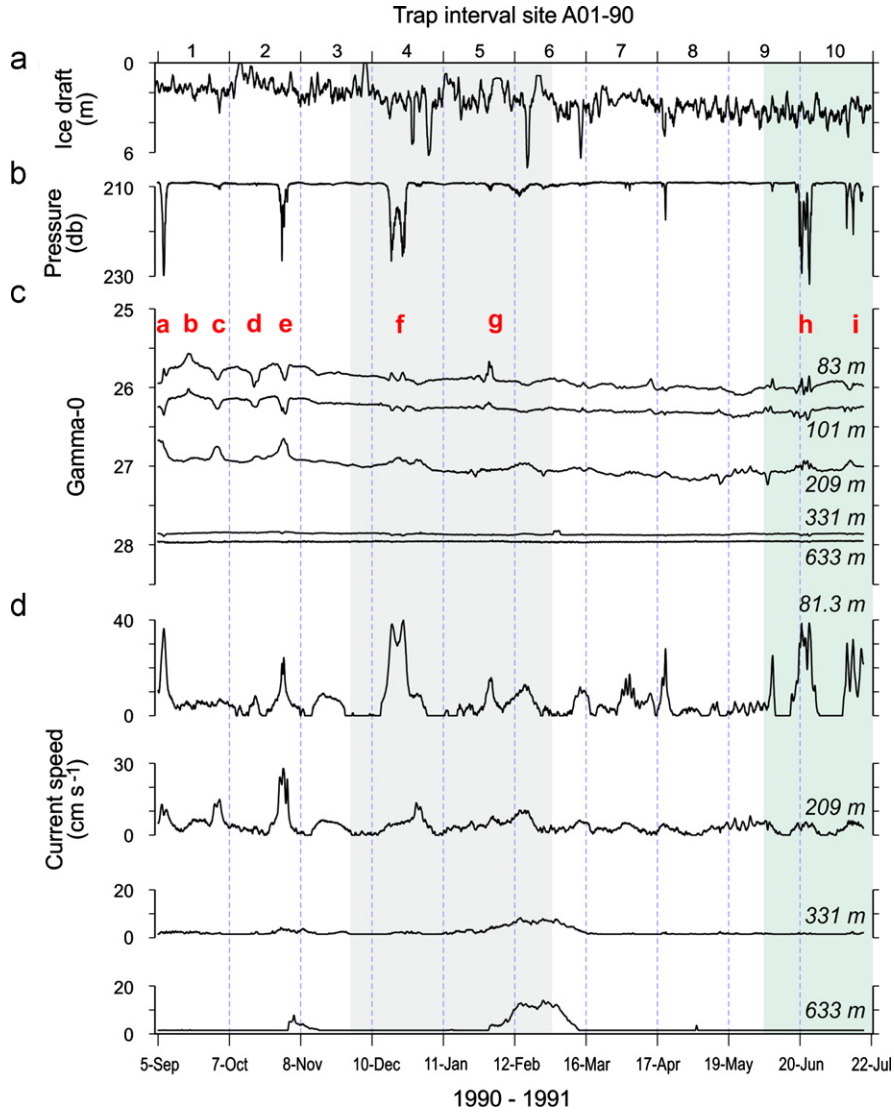

Fig. 4. Time-series physical data from mooring instruments for deployment at A01-90. The data are summarized in the following panels: (a) ice draft and ice presence from the upward looking sonar (ULS) at the top of the mooring; (b) pressure reading at one depth indicating where mooring pull-downs occurred in response to high current velocities; (c) density anomalies (gamma-0) at instrument depths; and (d) current speed records at instrument depths. Eddies discussed in the text are indicated by small case red letters at the top of the (c) panel. The light grey shaded area indicates winter (Dec–Feb) and the light green area indicates summer (Jun–Aug). The vertical gridlines indicate the sequential sediment trap sampling intervals.

above the speed maximum, doming for anti-cyclones and depression for cyclones. The resulting signature is a spreading of isopycnal surfaces at the core of an anti-cyclonic eddy and a pinching at the core of a cyclone (see Mizobata et al., 2002). In the presentation of Figs. 4–6, which displays time series of density at constant depth, the pinching and spreading signatures are interchanged: the curves pinch together (weaker vertical gradient of density) at the core of an anti-cyclone, and spread at the core of a cyclone.

Although our data from widely spaced levels of measurements do not provide well-resolved views of eddies, they are sufficient to identify an eddy's duration of impact at the mooring site. To make this clearer, we have adjusted the values of density to a constant depth to remove much of the spurious change caused by pull-down of the instrument into denser water by the fast current in eddies. Regrettably, the correction is no better than knowledge of the vertical density gradient within the eddy, which is difficult to determine near the level of maximum speed where gradients are most strongly perturbed. Our corrections are based on the gradient between instrumented depths measured by CTD when the mooring was deployed.

During 1990–1991 (see Fig. 4), five eddies passed A01during the first two trap intervals (events labeled a–e in panel c). Eddies were also present during trap intervals 4–5 (events f and g in panel c) at which time there was enhanced current down to 1517 m depth (data on plot only to 633 m). Two clear signatures occur near the end of the record during trap interval 10 (events h and i in panel c).

During 1992–1993 (see Fig. 5), four cyclonic eddies centered between 66 and 116 m crossed the mooring during the first three trap intervals (events j–m in panel c). The last of these eddies was most enduring and clearly spanned depths from 46 to 598 m. Two additional cyclonic eddies passed A01 later in the deployment, feature 'n' during interval 7, centered between 117 and 169 m and feature 'o' during interval 12.

During 1993–1994 (see Fig. 6), three eddies were obvious at the mooring. A weak eddy (event p in panel c) centered around 83 m appeared early in the fall of 1993. A very strong cyclonic eddy (event q in panel c; see also Fig. 7 panels a–d), centered between 83 and 140 m and extending from 61 to 265 m depth, arrived during trap interval 5; there is evidence that its outer edge was already touching the mooring during interval 3. It moved directly over the mooring in interval 6, causing large density perturbations and a classic signal in

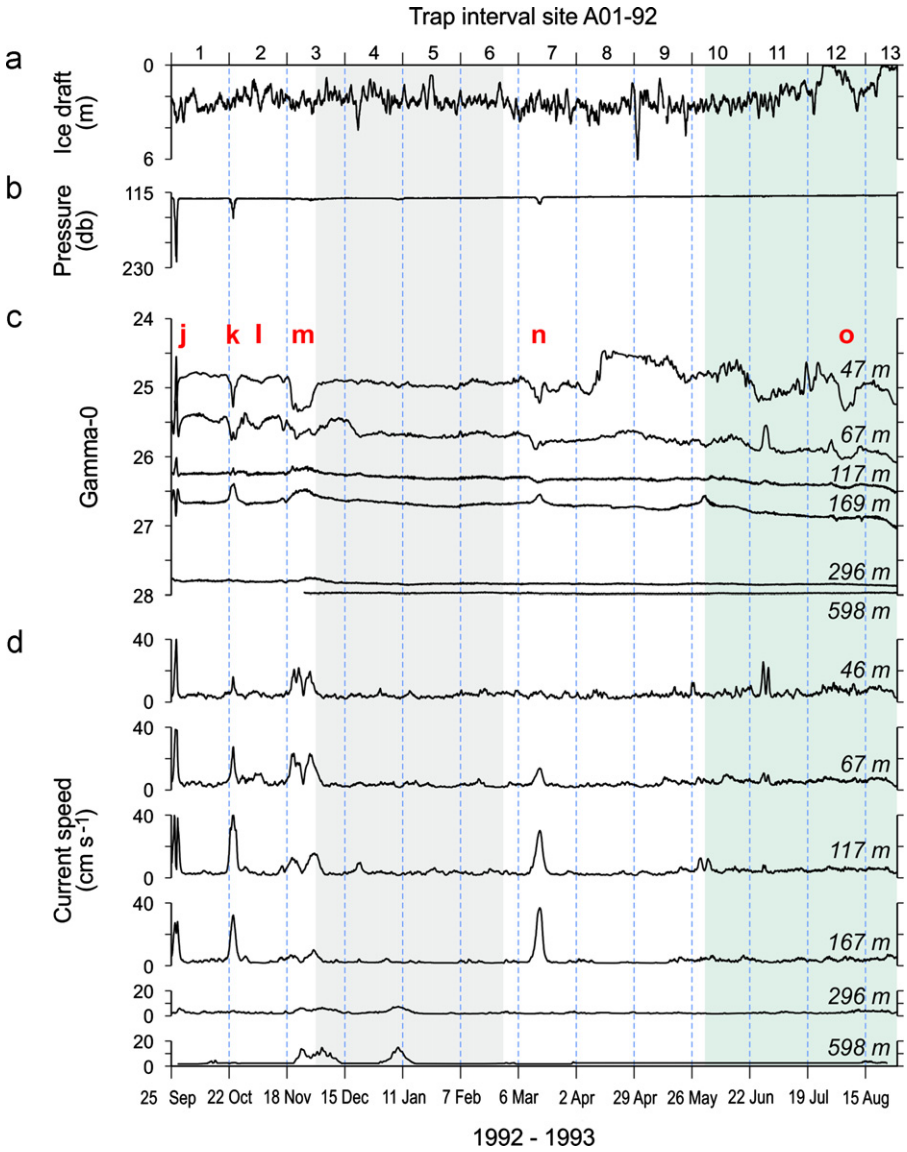

Fig. 5. Time-series physical data from mooring instruments for deployment at A01-92. See the caption for Fig. 4 for an explanation of the panels (a)–(d).

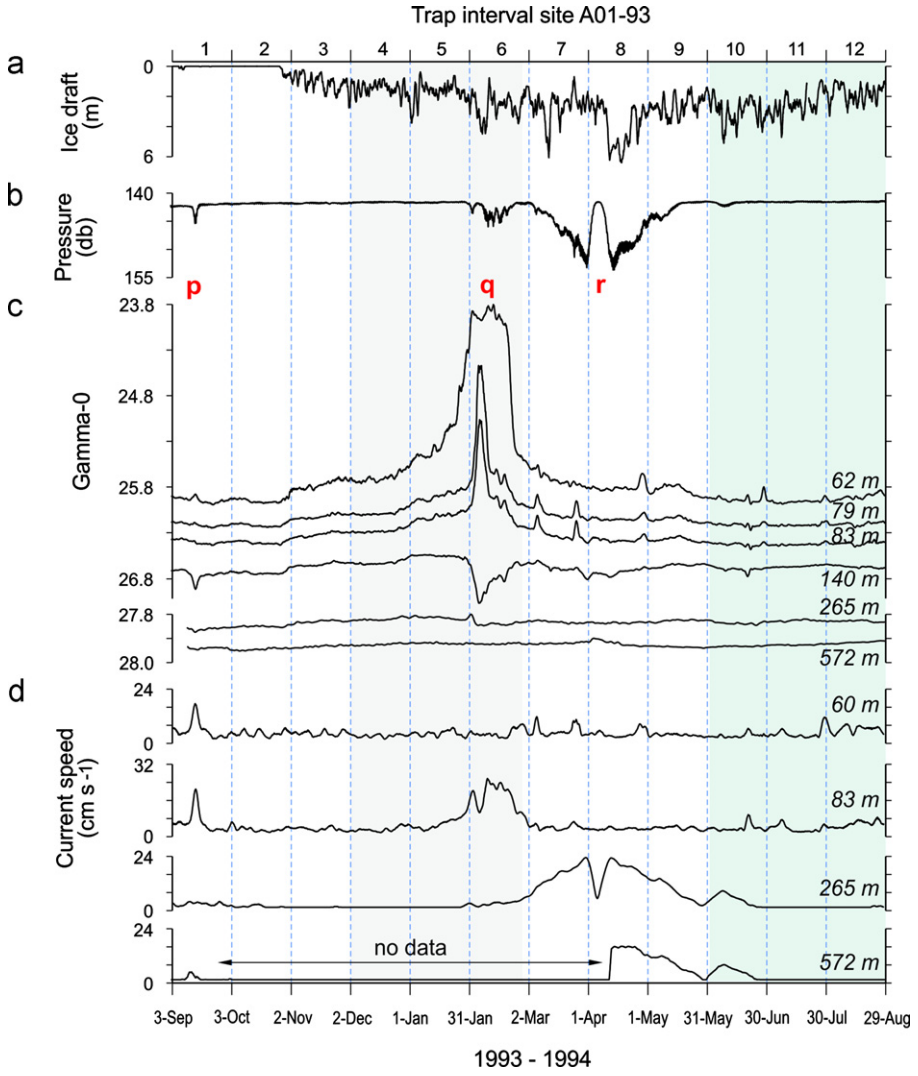

Fig. 6. Time-series physical data from mooring instruments for deployment at A01-93. See the caption for Fig. 4 for an explanation of the panels (a)–(d).

current speed—a strengthening, a dip to zero at the eddy's centre, an increase to a second peak and a final decrease as the eddy moved on. Fig. 7 panel d demonstrates that this cyclonic eddy's movement during intervals 5–6 was north-westward. Following the cyclonic eddy, an anti-cyclonic eddy (event r in panel c of Fig. 6; see also Fig. 7 panels a–c, and e) appeared at a much greater depth during intervals 7–8. Its presence is clearest in currents measured at 265 and 572 m and by the divergence of density values above 140 m from those below 572 m (Fig. 7 panel b). This anti-cyclonic eddy also passed directly through the mooring, as revealed by a minimum in current speed in interval 8. This appears to have been an anti-cyclonic eddy moving to the north-west (Fig. 7 panel e), although our identification of the sense of rotation may be equivocal because the judgment is based on rather small perturbations of density. These two eddies (events q and r) are depicted in more detail in Fig. 7: note that in Fig. 7 panel b, the density axis (gamma-0) is reversed from that in Figs. 4–6 to clearly display the pinching of the isopycnals at the core of a cyclone and visa versa for an anti-cyclone.

4. Regional environmental conditions during the study

Lithogenic particles settling in the Canada Basin come originally from rivers and eroded shore-lines along the perimeter of the Beaufort Sea. The mobilization of these particles and their transport across the shelf to the basin requires energetic phenomena and an appropriate direction of dispersal. Movement from source to sink may take some time. This section describes marine environmental conditions in the Beaufort region during the course of the study with emphasis on aspects that are relevant to the transport of small particles, namely prevailing winds and the occurrence of storms causing shore-line erosion, the timing and magnitude of the Mackenzie freshet (flow and particles), the timing of ice break-up and freeze-up and the presence and character of summertime pack ice. Summaries are presented in Figs. 8 and 9.

The first three panels of Fig. 8 display progressive vectors of surface wind during each of the operating periods at A01; the data come from the NCEP re-analysis at a nearby location (see Fig. 1). Each progressive vector diagram starts in mid-May, about three months before a mooring was deployed, and continues until mid-August of the following year, when trap collections were complete. Each vector represents one month that begins on the 15th of that month. The 1990–1991 operation was preceded by the equivalent of a 10,000 km wind push to west past the mooring site that started in mid-May, but conditions were relatively stagnant for 5 months after mid-July. An unusual eastward push equivalent to over 20,000 km past the site began in December, continuing to April when the direction reversed. These west-east oscillations during 1990–1991 were accompanied by a net

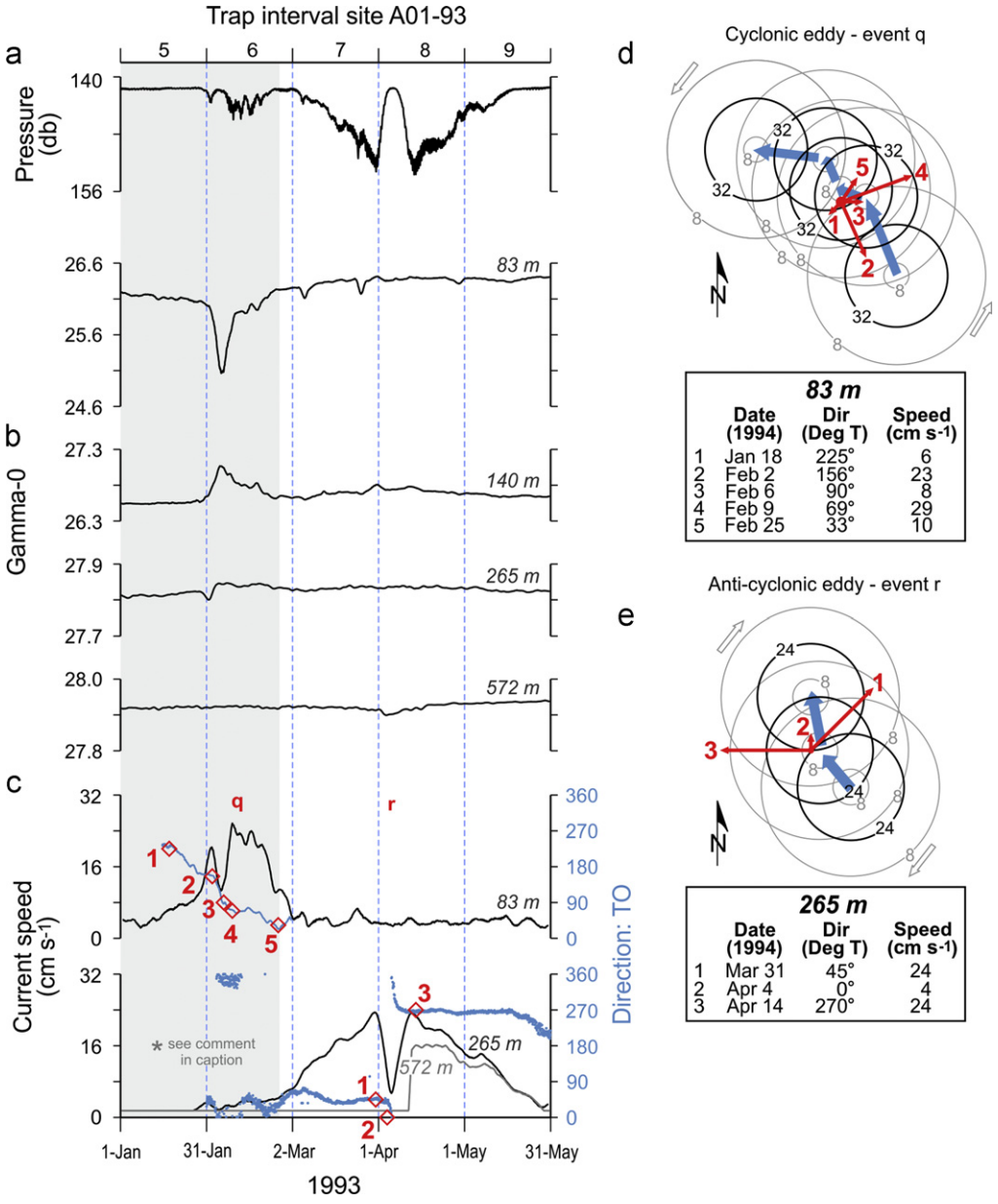

Fig. 7. Reduced and simplified version of Fig. 6 representing the cyclone in interval 5–6 and the anti-cyclone in intervals 7–8 of deployment A01-93; the intention is to clarify the orientation and direction of movement of these eddies with respect to the mooring. The figure is composed of the following panels: (a) pressure reading at one depth indicating where mooring pull-downs occurred; (b) density anomalies (gamma-0) at instrument depths; note that the axes for gamma-0 are reversed as compared to Figs. 4–6 to clearly show the pinching of the isopycnals for a cyclonic eddy and visa versa for an anti-cyclone; (c) current speeds (black lines) and current directions (blue lines); eddies are identified by the red lower case letters (q and r);. the red numbers and diamond symbols indicate specific points for which velocity vectors are drawn in the following two panels; (d) depiction of the motion of the cyclonic eddy (event q) as it passes over the mooring; and (e) depiction of the motion of the anti-cyclonic eddy (event r) as it passes over the mooring. In panels (d) and (e) the directions of eddy movement are indicated by the blue arrows; the dark rings represent the radius of maximum current speed and the light grey rings represent decreased current speeds at the inner and outer portions of the eddy; and the red arrows depict the velocity vectors at the numbered points indicated in panel (c). The tables in panels (d) and (e) specify the speed and direction of the current at the numbered points in panel (c). *Note that in the bottom plot in panel (c), only the current direction for 572 m is plotted because the direction data at 265 m was corrupted. Also note that only part of the 572 m current speed is plotted due to problems with the rotor at that depth. The assumption is made that the current direction at 265 m will be essentially the same as the direction at 572 m. (For interpretation of the references to color in this figure legend, the reader is referred to the web version of this article.)

southward impetus equivalent to 10,000 km past the site. During 1992–1993, wind conditions prior to the deployment were relatively stagnant, but a prolonged eastward push began in September which was equivalent to almost 35,000 km by March. Between this time and the end of the deployment A01-92, there was a strong return push to the west that cleared the ice off the shelves and created a vast expanse of open water out into Canada Basin. During the 1993–1994 operation there was very little net air movement. The push to the west that preceded deployment was followed by a slow over-winter return to the east. There was a modest south-westward push between April and July.

The last panel of Fig. 8 presents information on those winds having potential to erode the coastline bordering the Mackenzie shelf, namely strong north-westerlies in the late summer and fall. The bars display the fraction of time with wind from that quarter during August through October, when long ice-free fetch is most likely; this fraction varied little among the years. The three curves display the 80th, 90th and 95th percentiles of the square of wind

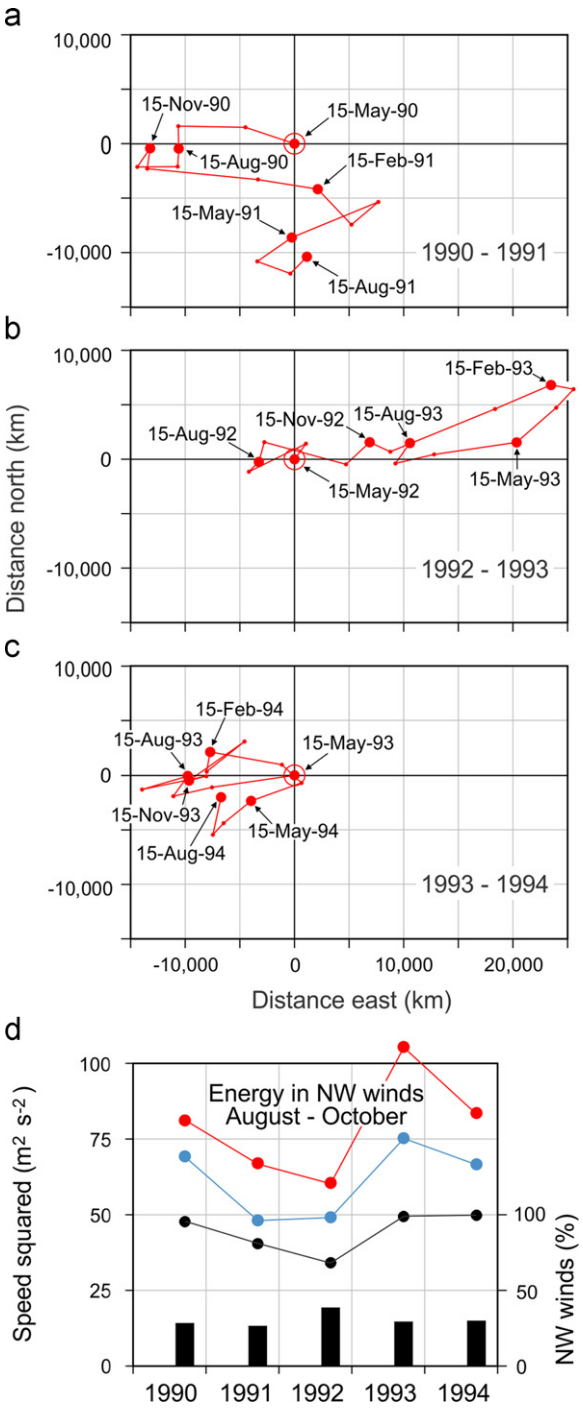

Fig. 8. Progressive vectors of surface wind during each of the operating periods at A01 (first three panels); the data come from NCEP grid point 71.426°N 140.625°W (see Fig. 1). Each vector diagram starts in mid-May, and continues until mid-August of the following year. Each vector represents a period of one month and begins on the 15th of that month (large red dots mark every 3rd month). In the last panel, bars display the fraction of time with wind from the northwest during August through October for each of the years (1990–1994) and the three curves display the 80th, 90th, and 95th percentiles of the square of wind speed (proportional to wind stress).

speed (proportional to wind stress). There is an almost two-fold variation in wind energy from a low in the summer of 1992 to a high in 1993.

Summertime ice conditions also differed greatly (Fig. 9). Prior to the 1990–1991 deployment, break-up began early in May on the Mackenzie shelf and by mid-August open seas prevailed to 71°N. The ice edge never reached A01, staying always south of 72°N and seas froze over in the second week of October. In 1991, break-up began early in May in response to the east–north–east wind at this time. However, the ice came back in after the wind reversed in July. In the summer of 1992, ice moved more quickly off shelf beginning at the end of June, reaching 71°N in mid-August (CIS maps). Break-up in 1993 was a little later than in 1990, but beginning in late May, ice cleared rapidly from the shelf and a wide adjacent area of the basin in response to sustained easterly wind. In 1993, a wide expanse remained clear of ice and freeze-up was late. Ice conditions in the summer of 1994 were intermediate, similar to those in 1992.

With a broad fetch to the north-west for several months and a greater incidence of strong wind from that quarter (Fig. 8), conditions in 1993 were favourable to the generation of large waves and consequent erosion of ice-bonded coastal bluffs and re-suspension of particles from the seabed (Manson and Solomon, 2007; Mulligan et al., 2010). However, such wind would generate current flowing eastward along the coast, so that re-suspended particles would initially be carried away from A01. It is conceivable that once reaching deeper water in Amundsen Gulf they may have been carried westward to A01 within the circulation of the Beaufort gyre. It is also possible that north-west gales created dense particle-laden layers very close to the seabed that flowed seaward as benthic density currents (Forest et al., 2007, 2008). Following an exceptionally long period of open water in the summer of 1987, and coinciding with a series of strong north-westerly wind events, O'Brien et al. (2006) observed a sudden simultaneous jump in flux of settling particles around the perimeter of Mackenzie shelf (at 50 m above the bottom at the 200 m isobath); an illustration of the sensitivity of the transport of resuspended sediments to strong wind events.

On the Mackenzie Shelf, it has been estimated that bottom current speeds (at 1 m elevation) of >19 cm s^{-1} are sufficient to resuspend the upper, less consolidated layer of bottom sediments and that speeds of >24 cm s^{-1} can erode the lower, more consolidated layer (O'Brien et al., 2011). Such current speeds have been observed and associated with resuspension in a number of circumstances in this area. During storms where orbital circulation of surface waves can be appreciable at the seabed in <10 m water, intense resuspension can occur (Hill et al., 1991). Intensifications of currents in the Beaufort shelf break jet have been associated with elevated levels of suspended particles (Forest et al., 2008) and variations in this energetic current may be conducive to the generation of eddies that incorporate and transport suspended particles into deeper waters (Spall et al., 2007). This and other studies (e.g., Krishfield et al., 2002) have observed currents in eddies that are easily high enough to erode bottom sediments if the eddy were to brush up against the slope or shelf edge. In addition, it is probable that during formation, eddies may incorporate particles that have been resuspended by other processes. Also related to wind events, Mackenzie Trough is a site of intense upwelling and generation of internal waves (Carmack and Kulikov, 1998); this may be also be a source of sediment resuspension and generation of nepheloid layers within the trough and along the slope (Cacchione and Drake, 1986).

There were also differences in the fate of fluvial inflow among the years of study (Fig. 9). In May 1992, the peak flow of the Mackenzie River – one of the highest ever – flowed onto a shelf still clogged with ice. In 1993, the freshet spread onto a shelf already clear of ice, and under the influence of an east wind, the river plume and its suspended particles were certainly driven north-west, following the ice. In 1991, the freshet arrived on a shelf only partly clear of ice, which continued to drift shoreward until September, blocking the river plume from reaching the

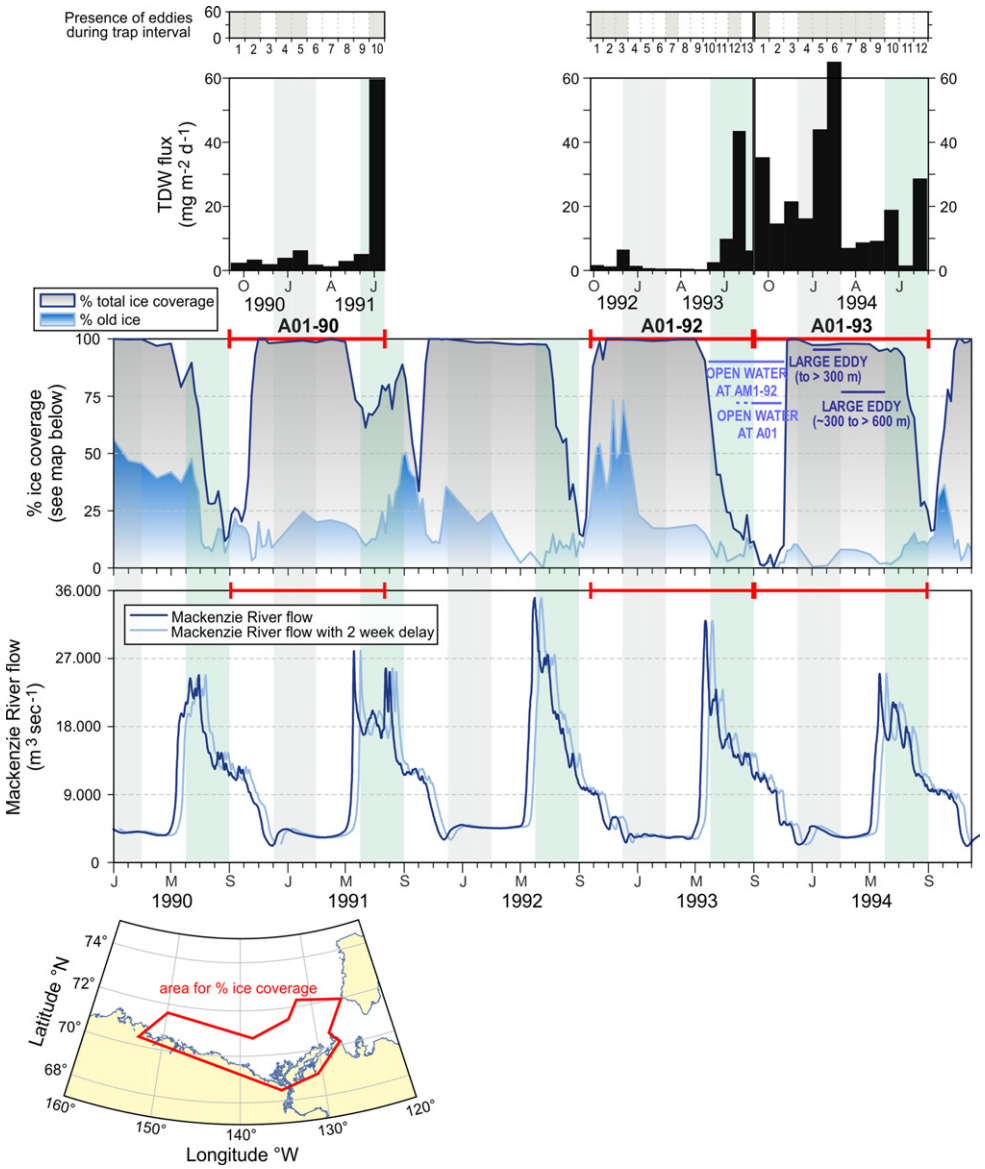

Fig. 9. Environmental conditions for the years 1990–1994 including the percent coverage of old ice and total ice on the Beaufort shelves (see inset map for area of coverage) and Mackenzie River flows at Arctic Red River (with a two-week delay assumed sufficient for the flows to travel ~250 km to the ocean); the mooring deployment periods at site A01 are shown at the top of each of these plots as red lines. The bar plots at the top depict the TDW fluxes at A01 and above the bar plots, the shaded intervals indicate the presence of eddies in a given trap interval. As in previous figures, winter (Dec–Feb) is shaded a light grey and summer (Jun–Aug) a light green. The periods of open water at sites AM1-92 (O'Brien, 2009) over the slope and at A01 in the Canada Basin are shown in the plot of % ice coverage along with the time periods coinciding with two large eddies (at the depths indicated) during the A01-93 deployment (these periods of open water and eddy occurrence are also depicted in Fig. 3a). (For interpretation of the references to color in this figure legend, the reader is referred to the web version of this article.)

basin. In 1994, the peak flows arrived when the shelf was still congested with ice.

5. Sedimentation in relation to environmental conditions

5.1. 1990–1991

Pack ice remaining on the shelf until mid-July 1990, long after the peak flow of the Mackenzie, likely confined the spreading plume and deposition of particles to an area close to Mackenzie Delta. Fetch limitation by pack ice and the relatively low incidence of strong wind from the north-west (Fig. 8) will have inhibited wave generation and the possibility of wave-driven sediment re-suspension from the seabed. The impetus of wind at this time was weak, promoting neither upwelling nor downwelling. In the fall of 1990 (trap intervals 1–3), the low TDW flux indicated a slow rate of particle delivery from the coastal Beaufort to site A01 (Fig. 2 and Table 2). Eddies that passed the mooring during the fall did not noticeably contribute particles to the traps at 615 and 1515 m (Figs. 2 and 4).

In mid-winter 1990 (trap intervals 4 to 6), the collections revealed an enhanced export of particles at a time when ice cover was complete and ice at A01 averaged 1–7 m in thickness. The trapped material was highly lithogenic, implying transport from the shelf. The wind was downwelling favourable for most of the 1990–1991 winter. If transmitted to the ocean, this wind stress might have forced particle-laden bottom water off the shelf, perhaps to reach A01. However, wind stress on an ice-covered ocean in winter can only be passed to the ocean via ice movement and eastward ice movement in the southern Beaufort is strongly impeded by ice stress generated against the mainland coast and

Banks Island (Williams et al., 2006); a strong downwelling response at this time is unlikely. The enhanced collection was coincident with and possibly linked to a series of eddies that passed the mooring at this time (Fig. 4). The TDW flux at the deeper trap was 4–6 times that at the shallower (Fig. 2a and b; Table 1). Unfortunately, our knowledge of eddy size and the distribution of particles and water properties within eddies is limited. If the flux sources were eddies, the difference between the two depths of collection perhaps reflects differences within eddies or among eddies, in attributes such as core depth, vertical extent, sense of rotation, speed of passage or particulate burden. For example, the eddy passing A01 during interval 4 was cyclonic with strong current and extended at least from 83 to 209 m depth whereas the event during interval 6 had strongest current much deeper, at 331 and 633 m.

In the summer of 1991, particles arriving with the Mackenzie freshet were likely deposited on the inner shelf near the Delta because the river plume was blocked by unusually dense pack ice on the outer shelf (Macdonald et al., 1995). Ice-limited fetch would have suppressed wave-induced resuspension of particles from the seabed that summer. However, despite A01's isolation from the earlier freshet and its 2–3 m of ice, there was a peak in particle flux at 615 m in July (interval 10; Fig. 2); this was coincident with the passage of two eddies within the halocline (83–209 m; current to 40 cm s^{-1}), The material in the peak had high LITH content and higher POC content (6.2%) than normally found in shelf sediment. Its low fluxes of CHLA and PHAEO suggest an absence of contributions from phytoplankton production earlier in the year.

5.2. 1992–1993

In 1992, dense pack ice remained south of 71°N until mid-August, 10 weeks after freshet. This ice barrier likely confined the plume and fluvial sediments to the inner shelf near the Delta. It is probable that primary production was also relatively low, by reasons of the containment of fresh water (suppressed upward mixing of nutrients) and of light limitation by ice. A01 was covered by 2-m ice when the mooring was deployed (25 September 1992) and remained under 1–3 m ice all winter. Ice actually cleared from A01 in 1993, in the third week of July.

The low flux of particles at A01 during the fall and winter of 1992–1993, except for a small 4.5 mg m^{-2} d^{-1} peak during interval 3, may reflect these heavy ice conditions (Fig. 2). Several eddies crossed the site during intervals 1–3 (Fig. 5) but only the eddy in interval 3 coincided with enhanced particle flux; this anticyclonic eddy passed directly through the mooring, was centered near 100 m, and spanned 47–296 m.

The clearance of ice in the summer of 1993 was early and extensive, and freeze-up was not complete until early November. The freshet of the Mackenzie occurred at the end of May, when ice was clearing rapidly to the north-west in response to persistent east wind. The buoyant plume would likely have responded similarly, spreading far beyond the shelf to the north-west. Elevated biogenic and lithogenic fluxes at A01 between mid-July and mid-August (trap interval 12) may reflect both north-westward dispersal of the Mackenzie River plume and primary production across the wide expanse of open water. Most importantly, in the extensive open water period in 1993, the elevated lithogenic fluxes at A01 may echo the increased wind energy (Fig. 8d) available for processes that resuspend and transport sediment over the shelf and slope.

Peaks in both biogenic and lithogenic fluxes at A01 in the late summer of 1993 (interval 12) were coincident with open seas. Elevated CHLA and PHAEO fluxes at this time suggest that the biogenic material came from phytoplankton production close to A01 (and the ice edge) with relatively quick delivery to the trap. The elevated pigments in this biogenic peak are unique in the record, different from the low pigment fluxes in the summer of 1991, although both were accompanied by peaks in lithogenic material. In part, the lithogenic fraction, although originally from the shelf or slope, may to some degree, have been swept up in the downward rain of biogenic material from the euphotic zone and hence delivered more quickly to the trap. The 1993 peak in summer coincided with a small peak in OPAL flux, indicating that the biogenic material contained diatom frustules.

At the end of August 1993 (between the recovery of A01-92 and the deployment of A01-93), CTD casts were done at site A01 and sites to the south over the slope (see the Supplemental material for map and plots of the data). Two of the casts higher on the slope – one to the west of the mouth of Mackenzie Trough (at 580 m) and the other to the east of the Trough (at 657 m) – exhibited nepheloid layers throughout the water column and anomalous temperature and salinity profiles as compared to site A01. During the same period, another cast north of these sites (at 1329 m) exhibited decreased percent transmission (as compared to site A01) from about 270 m to the bottom of the cast at 1700 m; a possible indication of widespread presence of suspended particles over the slope. In addition, there was a fluorescence peak at about 42 m in one of the casts at A01 and at the 1329 m site over the slope; a confirmation that primary productivity (albeit patchy at A01) in the ice-free surface waters over the deep basin may have been the source of the high pigments in the trap sample collected in July–August 1993 at 600 m; evidence that under some circumstances the biological pump may function over the Canada Basin. Unfortunately, similar CTD data is not available for the other years which were subject to different conditions of wind and ice.

5.3. 1993–1994

Ice cleared early from the southern Beaufort Sea in 1993, so that a broad ice-free expanse extended far beyond the shelf by the time the 1993–1994 mooring was set out in early September. There were occasional incursions of 3-tenths pack ice at A01, but the edge of compact ice was well to the north at about 74°N. Freeze-up was not complete until early November. Thereafter, A01 remained under ice until the end of the trap collection in late August 1994.

Open-water fetch was large during the summer and fall of 1993. With this fetch, strong wind from the north-west would be an effective agent for resuspension of sediment from the seabed in shallow water and for mobilization of new material by wave erosion of the shoreline (Manson and Solomon, 2007). Previous study has demonstrated a connection between enhanced downward particle flux at the shelf edge and cross-shelf particle transport within a bottom nepheloid layer under such weather and ice conditions (O'Brien et al., 2006).

Mackenzie River inputs peaked at about the same time in 1994 as in 1993 but the peak flow was lower. In contrast to 1993, the 1994 freshet occurred when ice was still land-fast around the Delta and much of the shelf was choked with first-year pack ice. Under these conditions, the fresh water and its load of fluvial particulates was likely contained in shallow areas, as in 1992.

In the fall of 1993 (intervals 1–4), the biogenic and lithogenic fluxes remained elevated but variable while the lithogenic content declined from 75 to 64%. In September 1993 (interval 1), peaks in lithogenic and biogenic material coincided with an eddy centered above 140-m depth and spanning 60–572 m (Fig. 6). Fluxes were again elevated during intervals 2 and 4 (October, December) at times when the records of density suggested that

the outer edge of a strong eddy, later to cross the mooring, was just touching it (Fig. 6).

Early in 1994 (intervals 5, 6), a strong cyclonic eddy moved across A01, apparently from south-east to north-west (Fig. 7d). This eddy coincided with increased fluxes of both biogenic and lithogenic material. The composition of the material trapped during these two intervals appears to be unique – elevated LITH content, BIOSI:POC ratio and pigment flux along with low POC content (Fig. 3). This feature is a good example of the capacity of eddies to transport particulate material from the shelf or slope far out into Canada Basin. High levels of CHLA and PHAEO within the mid-winter peak are surprising and may be evidence of primary productivity within the eddy as it moved through ice-free seas in the fall of 1993. Alternatively, the elevated pigments may be evidence of detritus from standing stocks of primary production delivered to the seabed on the slope and later remobilized perhaps via impingement of the eddy's strong current on the seabed there.

Biogenic and lithogenic fluxes abruptly decreased in March 1994 (interval 7), coincident with a change in composition—dramatically decreased LITH, OPAL and pigment contents and increased POC. A deep eddy was crossing the site on a north-west trajectory at the same time (trap intervals 6–7)—anti-cyclonic, centered between 140 and 572 m with strong flow at 265 and 572 m. This eddy remained close to the site during intervals 7–9.

Current was also strong at 265 and 572 m during interval 10 (Fig. 6). This occurrence may have been linked to the same eddy, since the composition of the material collected during interval 10 is the same for intervals 7–9. The biogenic material for these intervals was unaccompanied by pigments, suggesting either that it was not the outcome of primary productivity, or if it was that the material was degraded. There were also at least four smaller eddies in the upper halocline during intervals 7–10, which were independent of the larger feature in the lower halocline; all may have contributed to the fluxes.

There was another change in the composition of trapped material in July–August 1994 (intervals 11, 12), but no clear signatures of eddies; currents at 60 and 83 m increased slightly. The change in composition involved increases in % LITH from 72 to 81%, in BIOSI:POC molar ratio and in PHAEO flux (but not CHLA flux). This signal suggests that the biological material was likely a remnant of older production that had moved with lithogenic material from the shelf or slope.

The enhanced lithogenic and biogenic fluxes at A01 during 1993–1994 coincided with and followed the unusually open ice conditions, sustained south-east wind and clear skies in the summer of 1993. However, our data also exhibit clear links between the presence of eddies and changes in composition and fluxes of suspended particles.

6. Summary and conclusions

We have studied particle fluxes in the Canada Basin and explored the physical processes that transport particles to and within deep Arctic Basins. This study was conducted during the period 1990–1994 prior to the recent decline in Arctic summertime ice and as such provides an important baseline for future studies. Although for most of the global surface ocean, the biological pump is the primary means for delivering POC to the abyssal depths and the seafloor (Honjo et al., 2008), it has been hypothesized that this mechanism is essentially not applicable to the interior Arctic Ocean where the primary production does not reach traps at 100 m (Honjo et al., 2010). Despite this, particles are trapped deep in the water column (this study and Honjo et al., 2010) and are ultimately exported to the seafloor of the deep basins (Stein and Macdonald, 2004). Lateral transport of resuspended particulate material from the basin margins to the deep ocean has been hypothesized but the specific processes involved are not well understood. Our deep ocean time-series sediment trap experiment supports this hypothesis of an ineffectual biological pump over the Canada Basin and demonstrates that eddies originating over the shelf/slope regions are one means of entraining resuspended sediments and transporting them laterally over great distances where they are dispersed over the deep basin.

The annual export pattern seen by both this study and by WHOI (site CD04; Honjo et al., 2010) confirms that particle export in the Canada Basin is unrelated to seasonality trends observed globally. This is perhaps not surprising in light of the unique characteristics imprinted on the Arctic Ocean by the disproportionate influence of vast continental shelves, coastal erosion, massive riverine inputs (freshwater and particulates), and extreme fluctuations in ice cover, light and temperature. In this study, the absence of an obvious pattern of seasonal variation in particle flux is reflected by the lack of a consistent pattern of seasonal variation in forcing factors – wind, ice cover, ice drift, and river inputs – in this region.

Ice conditions in the summers varied markedly and although there was a summer peak in particle flux during each deployment, the compositions and likely sources of the particles varied. In 1991, heavy ice remained over the Beaufort Shelf in summer and the highly lithogenic composition of the summer peak was consistent with lateral transport of resuspended shelf/slope sediment and not with vertical transport via the biological pump. In 1993, a vast expanse of open water extended from the shelves far out into the basin and the composition of the summer peak was consistent with a combination of lateral transport of resuspended shelf/slope sediments and in a limited way, the biological pump. The high pigment fluxes during the summer peak in 1993 – by far the highest in the dataset – coincided with the only prolonged ice-free period at A01 during the study period. In contrast, a major ice opening during a 2004–2005 study by Honjo et al. (2010) did not have a significant impact on fluxes in the deep Canada Basin (site CD04-3067 in Fig. 10), indicating that, in this case, local surface primary production if present was not transported vertically via the biological pump.

Caution is advised when suggesting sources of biogenic material collected in the traps. In this study, analysis of the pigment content was useful in identifying contributions from primary productivity or standing crops of phytoplankton. The high lithogenic content of many of our samples implies that refractory organic carbon (terrigenous or marine) constitutes a significant proportion of the captured carbon. In future studies, it is important to distinguish the proportions of the carbon flux attributable to biological production (autotrophic and heterotrophic) and to refractory organic carbon (terrigenous or marine). Honjo et al. (2010) used $\Delta^{14}C$ values to distinguish a predominance of contemporary carbon in sea-ice tethered traps (at 120 and 200 m) from the pre-aged organic carbon collected in the deep trap at 3067 m (see Fig. 10).

An average of six baroclinic eddies crossed the A01 mooring site each year and both cyclonic and anti-cyclonic eddies were observed. The highest TDW flux peaks in the record all coincided with the presence of eddies and the majority of the TDW flux peaks higher than 10 mg m^{-2} d^{-1} were concurrent with an eddy. Some lower peaks were similarly linked to eddies, but some eddies had no discernible impact on the TDW flux.

Higher current velocities usually lead to under trapping of settling particles (Buesseler et al., 2007 and references therein) whereas, in this study, fluxes during intervals coincident with eddies and hence higher current velocities exhibited enhancements ranging from two- to ten-fold—evidence that higher fluxes

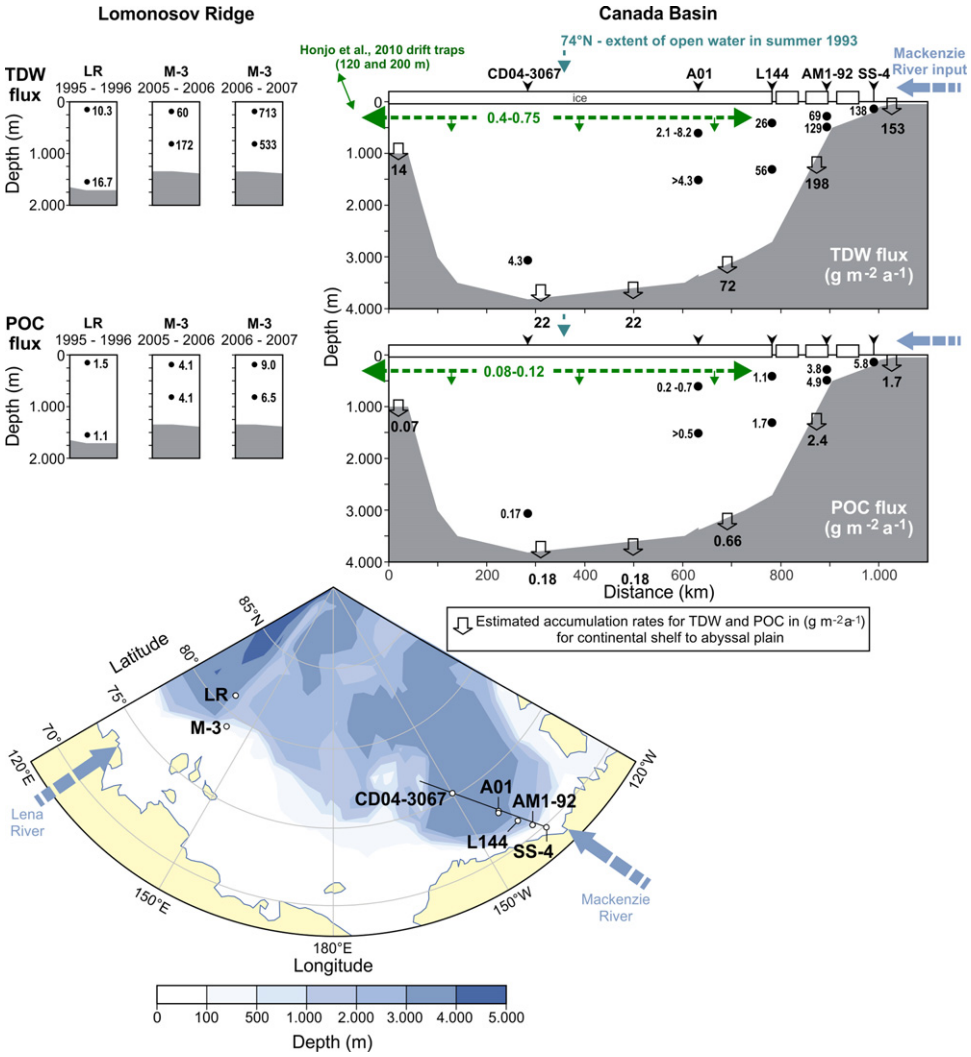

Fig. 10. Cross-sections of the Canada Basin depicting TDW and POC fluxes (in g m^{-2} a^{-1}) measured by sequential sediment traps at sites CD04-3067 (Honjo et al., 2010), A01 (this study), L144, and AM1-92 (O'Brien, 2009), and SS-4 (O'Brien et al., 2006). Also shown on the cross-sections are ranges of fluxes (TDW and POC; in g m^{-2} a^{-1}) from traps at 120 and 200 m that drifted with the ice in Canada Basin (Honjo et al., 2010; see green dashed line). For a comparison, TDW and POC fluxes (in g m^{-2} a^{-1}) for two sites on the Lomonosov Ridge are depicted to the left of the Canada Basin cross-sections; M-3 (Lalande et al., 2009) and LR (Fahl and Nöthig, 2007). Map shows locations of the sites. Accumulation rates (in g m^{-2} a^{-1}) of TDW and POC in the bottom sediments are indicated in the *x*-section for the Canada Basin for Arctic shelves, slopes, rises and abyssal plains (derived from Stein and Macdonald, 2004 (Table 8.3 page 319)). (For interpretation of the references to color in this figure legend, the reader is referred to the web version of this article.)

occurring when eddies were present must result from higher concentrations of particles in the eddies. In addition, the degree to which fluxes are enhanced reflects the fraction of the trap interval during which eddies were present. The highest TDW flux peak in the whole record was concurrent with an eddy that stayed over A01 for most of the trap interval (February 1994). Another high peak (in July 1991) was linked to two eddies that together spanned half the trap interval. The third highest peak (in July 1993) coincided with a weak eddy at the site for half the trap interval.

Dramatic compositional differences in trapped sediments were associated with specific eddies as exhibited by an abrupt change in composition that occurred in the winter of 1993–1994 as two distinct eddies passed over the mooring. The biological material in the mid-winter peak (January–February 1994), coincident with a persistent eddy in the halocline, exhibited evidence of the export of standing crops of phytoplankton indicating entrainment of surface water by the eddy or that the eddy itself provided favourable circumstances to support a fall bloom. In contrast, during the subsequent intervals (March–April 1994), a much deeper eddy passed over the mooring and although the exact origin of the biogenic material is unknown, its composition was clearly distinct from the biological material in the previous two intervals. In both cases we see the interplay between ice cover and eddies as the means to transport or produce particles.

The TDW flux throughout the fall and winter of 1993–1994 was vastly higher than that during either of the other two winters. This unusual wintertime period of high TDW flux followed unusual weather and ice conditions in the summer of 1993, when seas at A01 were clear of ice and prevailing east wind drove the Mackenzie River plume out there. However, it also coincided with an unusually persistent eddy at the site. There is not sufficient information to decide the cause, but the strong link between eddies and particle flux elsewhere in the three-year record does tip the balance away from a fluvial contribution to this mid-winter peak.

Recognizing the limited availability of data for Arctic Ocean Basins and in order to put our data in perspective, we have assembled a cross-section of particle fluxes in Canada Basin from our measurements and other published data (Fig. 10). The average

annual flux of particles at 600 m depth in the southern Canada Basin is low (4.2, 2.1, and 8.2 g m^{-2} a^{-1}; this study) compared with other world ocean basins, but consistent with existing data for the Arctic. Particle fluxes at site A01 are comparable to those from 3067 m in the Canada Basin (4.3 g m^{-2} a^{-1}; Honjo et al., 2010) but are significantly larger than particle fluxes from sea-ice tethered traps in the upper ocean (120 and 200 m) over the deep areas of Canada Basin (0.4 to 0.7 g m^{-2} a^{-1}; Honjo et al., 2010 see Section 4.1; Fig. 10). Mid-water TDW fluxes increase dramatically over the Beaufort slope to the edge of the continental shelf—26 to 138 g m^{-2} a^{-1} (see transect in Fig. 10; O'Brien et al., 2006; O'Brien, 2009).

The continental slope adjacent to the Lomonosov Ridge provides a useful comparison to the Canada Basin/Beaufort Sea area in that both are influenced by large river inputs and by varying sea ice cover. Over the slope adjacent to the Lomonosov Ridge, Fahl and Nöthig (2007) report lower annual fluxes of TDW but very similar POC fluxes compared to those reported at similar depths on the Beaufort slope (Fig. 10; site LR). As suggested by Fahl and Nöthig (2007), this may reflect the closer proximity and therefore larger influence of Mackenzie River inputs to the Beaufort Slope. In addition, their trap data reflect variations in ice cover and suggest the occurrence of a lateral sediment flux below the deepest trap. Lalande et al. (2009) report annual fluxes of TDW and POC (Fig. 10 site M-3) in the Laptev Sea for two years of differing ice covers; the second year (2006–2007) had a record low in Arctic ice extent. Lalande et al. (2009) attribute the increases in TDW and POC fluxes in the low ice year to an increase in marine primary production over the Siberian shelves (determined on the basis of Satellite-derived chlorophyll *a* concentration data). While this conclusion is supported by the satellite data, the decrease in % POC (to 1.2–1.3% POC of annual TDW flux) in (2006–2007) along with the large increase in TDW flux suggests that most of the increase in POC flux in this year was from refractory carbon (terrigenous or marine) associated with the lithogenic fraction and not from enhanced primary production. Notably, the TDW and POC fluxes in both years of the Lalande et al. (2009) study do not increase with depth as was observed in both this and the Fahl and Nöthig (2007) studies. This may be due to a much greater influence of the buoyant plume from the Lena River at the M-3 site. These examples and observations during our study demonstrate that success in understanding sediment transport in the Arctic Ocean depends on expanded spatial and temporal sampling regimes and an in-depth understanding of the over-all environmental conditions that prevail during the sampling periods.

Over the Holocene, estimates of accumulation rates of total sediment from the shelf to the deep basin (Stein and Macdonald, 2004; derived from Table 8.3, p. 319) are consistently in excess of the annual fluxes at the trap sites (Fig. 10; x-section of TDW flux). This indicates that a significant portion of sediment accumulating at the bottom must be transported close to the sea floor and consequently is not accounted for within the vertical expanse over which sediment traps have been deployed. Accumulation rates of organic carbon on the other hand are more comparable to the POC fluxes at the trap sites moving from the continental slope to the deep basin and notably are virtually identical in the deep basin. On the upper slope and on the continental shelf, the POC fluxes measured at the trap depths exceed the accumulation rates in the sediments indicating that the excess POC is either swept into deeper waters and metabolized before reaching the sediments or it is deposited and metabolized by the benthos.

The trap collections were dominated by lithogenic material, which is traceable to the eroded material delivered either by rivers or via erosion of the coastline and shelf/slope. Collectively, our data support the hypothesis of lateral transport of highly lithogenic resuspended material from the surrounding margins as a dominant process for the Arctic Ocean. In the deep Canada Basin (site CD04-3067 in Fig. 10; Honjo et al. (2010) observed a tight coupling between aluminum and organic carbon fluxes along with a lack of correlation between enhanced exports and specific seasons of the year; this led to the conclusion that export fluxes were driven primarily by physical forcing phenomena and not the biological pump. This tight coupling was also observed at site L144 (see Fig. 10) in material collected at 1311 m (2700 m water depth) over a full annual cycle (O'Brien, 2009).

Numerous studies, in a wide range of marine environments, have demonstrated that lateral transport of resuspended sediments may play a more important role in the global ocean carbon cycle than has previously been recognized (Hwang et al., 2010). Given the vast areas of continental shelves surrounding the deep Arctic Ocean basins, the influence of lateral transport on the carbon cycle in the deep Arctic Ocean basins is likely magnified compared to other deep ocean basins. This study demonstrates that the lateral transport of suspended particles within passing eddies can enhance the export of particles at mid-depths over deep Canada Basin but many questions remain regarding: (1) processes important to sediment resuspension at the basin margins, (2) eddy formation and entrainment of resuspended particles, (3) mass balance of settling particles within and over the lifetime of the eddy, and (4) other mechanisms capable of lateral transport from the margin to the deep basin.

Although measurements of beam attenuation by vertical profiling may miss the presence/flux of large particles, a cross-section over the slope seaward of the Mackenzie Shelf demonstrates the dynamic nature of processes occurring at and beyond the shelf edge in this region (Fig. 11a–f). In this cross-section, elevated concentrations of particles are evident in the surface layer, in a thick bottom nepheloid layer at the shelf edge, and close to the bottom over the slope. In addition, particle concentrations are elevated in the core of a cold core anti-cyclonic eddy centered at about 100 m and spanning the top 400 m of the water column; this eddy exhibits anomalous oxygen and nutrient concentrations as compared to the adjacent casts (see cast 69 in Fig. 11 a–f; nutrient data not shown). This eddy was at the 1100 m isobath and may be poised to transit into Canada Basin along with its anomalous properties and load of suspended particles. The strong fluorescence signal seen at about 35–49 m in cast 69, may indicate a strong phytoplankton bloom facilitated by upwelling of nutrients within the eddy (see cast 69 Fig. 11b). Considering that eddies are a frequent of occurrence in the Canada Basin, it is important to consider possible effects of eddy-driven upwelling in the increasingly ice-free waters over the basin (e.g., see McGillicuddy et al., 2007). Although not as clear as the eddy within the halocline (cast 69, Fig. 11), the pinching of the isopycnal lines at approximately 750 m at cast 70 may indicate the presence of a cyclonic eddy. Fig. 11 demonstrates the need to better understand the connection between sediment resuspension processes at the basin margins and the processes that transport resuspended particles to the deep basins.

Although eddies are ubiquitous in Canada Basin and the Beaufort Sea (Krishfield et al., 2002 and references therein), much remains unknown about their formation at the basin margins and their evolution (track followed, dissipation rates, and fate of biogeochemical materials transported within them). On the Chukchi Sea continental slope, a cold-core, anti-cyclonic eddy similar to the one depicted in Fig. 11 – with a diameter of ~16 km and an age in the order of months – exhibited elevated levels of nutrients, organic carbon, suspended particles, and shelf-derived neritic zooplankton compatible with a shelf edge origin. This eddy was likely on the brink of transiting from the slope to the deep waters over the Canada Basin (Kadko et al., 2008;

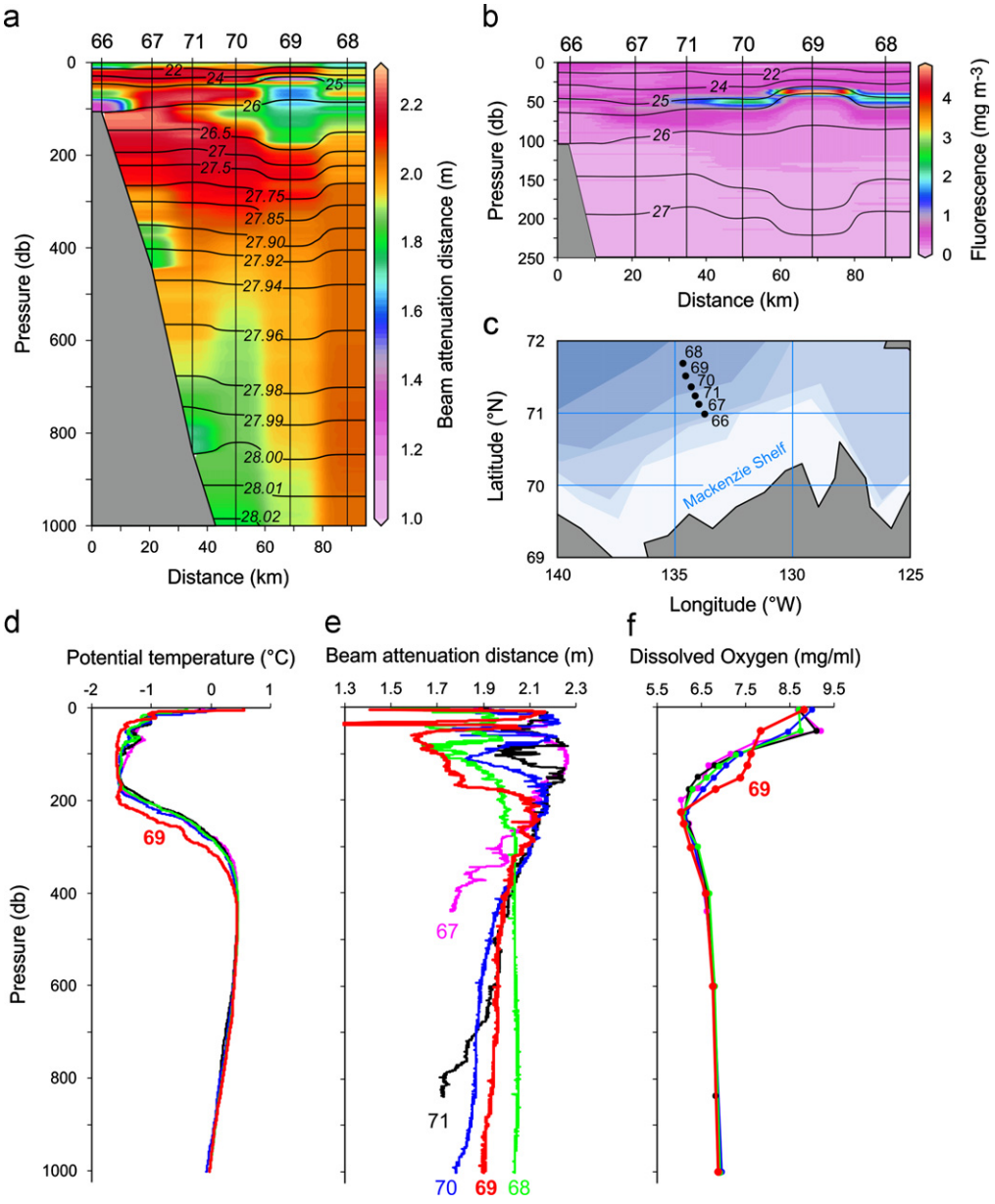

Fig. 11. Hydrographic cross-section from the edge of the Mackenzie Shelf out to the 1500 m isobath. The CTD transect was conducted on September 13–14, 2003 and the data is from the Institute of Ocean Sciences data archive. The bottom depths of the six casts are as follows: cast 66 (106 m), cast 67 (444 m), cast 71 (833 m), cast 70 (1140 m), Cast 69 (1100 m), and cast 68 (1522 m). Measurements were done using a Sea-Bird CTD (SBE-25) instrument and transmissivity readings were converted to beam attenuation distance units (m). Dissolved oxygen concentration was determined using an automated titration system consisting of a Brinkman dosimat (model 665) and a PC 900 Colorimeter.

Mathis et al., 2007). Direct measurement of eddy dissipation rates and trajectories in the Arctic Ocean are rare (Kadko et al., 2008; references therein) due to the harsh field conditions but it is important to track eddies such as these over time in order to properly understand their significance to the carbon cycle in the Canada Basin. Using reasonable estimates of particle loads, O'Brien (2009) estimated that an eddy could sustain a particle rainout for up to ~4 months over a trajectory of 100–500 km (for eddy drift speeds ranging from 1 to 5 cm s^{-1}). To put this in perspective, site A01 is ~350 km from the mouth of Mackenzie Trough and the maximum TDW flux at site A01 was ~65 mg m^{-2} d^{-1}.

Episodes of high particle flux in the Canada Basin are short-lived and can obscure signals of longer seasonal and inter-annual period. From 1990 to 1994, our moorings sampled three complete winter seasons but only one complete spring/summer/fall period (1993) and this limits our knowledge of inter-annual and seasonal variability. Due to the highly episodic nature of events in the Arctic, the use of shorter collection intervals in future studies will help resolve variability and its environment context. Peaks in particle flux at different depths in the water column are not necessarily coincident and so, data from a single depth cannot be used with certainty to extrapolate to other levels.

We conclude that the inter-annual and seasonal variations in fluxes at 600 m depth in the Canada Basin are broadly controlled by degree of ice cover and presence of eddies. Eddies formed in seasons with extensive areas of open water such as the summer of 1993 appear to entrain more resuspended material than eddies formed during years of heavy ice over the slope and shelf as occurred in 1992 and 1994 (and to a lesser extent in 1990). The increase in particle flux with depth (at A01-90) highlights the importance of sampling the water column at several depths to

resolve the mechanisms and pathways by which sediments are transported to the interior Canada Basin. Key factors that appear important to this transport are: (1) the ice cover extent on the shelves and timing of that extent with respected to river freshets and wind forcing; (2) the location and availability of readily resuspended sediments; (3) the co-occurrence of eddy formation with abundance of resuspended particulates; and (4) primary production. For example, in 1992, ice held the peak Mackenzie River inputs of freshwater and suspended sediment closer to the coastline restricting its further transport. In contrast, in 1993, the plume freely expanded into open water over and beyond the shelf at the time of the peak inputs. Open water also facilitates resuspension by winds and coastal erosion by waves, both of which feed the supply of transporting sediment (Manson and Solomon, 2007). Our data strongly suggest that open water over the shelf and slope is conducive to off-shelf transport of suspended particulate material—particularly when expanses of open water coincide with high influxes of suspended particles from rivers, coastal erosion or resuspension of shelf sediments. It is important to note that enhanced particle fluxes in winter have been reported over the Mackenzie slope and all coincided with elevated current speeds (Forest et al., 2007, 2008; O'Brien et al., 2011) implying that under the right conditions it is possible that transport of sediments to the deep basin may also be initiated under complete ice cover as well as during open water conditions.

Acknowledgements

We acknowledge our collaborators Knut Aagaard (then at Pacific Marine Environmental Lab, Seattle) and Richard E. Moritz (Applied Physics Lab, University of Washington). The project was funded in Canada by the Northern Oil and Gas Action Plan (NOGAP). Special thanks to the Canadian Coast Guard and the Polar Continental Shelf Project for logistical support and to our many colleagues involved in the collection and analysis of these data.

Appendix A. Supporting information

Supplementary data associated with this article can be found in the online version at http://dx.doi.org/10.1016/j.dsr.2012.10.004.

References

Aagaard, K., Andersen, R., Swift, J., Johnson, J., 2008. A large eddy in the central Arctic Ocean. Geophys. Res. Lett. 35, L09601, http://dx.doi.org/10.1029/2008GL033461.

Anderson, L.A., 1995. On the hydrogen and oxygen content of marine phytoplankton. Deep-Sea Res. Part I 42, 1675–1680.

Ashjian, C.J., Gallager, S.M., Plourde, S., 2005. Transport of plankton and particles between the Chukchi and Beaufort Seas during summer 2002, described using a video plankton recorder. Deep-Sea Res. Part II 52, 3259–3280, http://dx.doi.org/10.1016/j.dsr2.2005.10.002.

Baker, E.T., Milburn, H.B., 1983. An instrument for the investigation of particle fluxes. Cont. Shelf Res. 1, 425–435.

Buesseler, K.O., Antia, A.N., Chen, M., Fowler, S.W., Gardner, W.D., Gustafsson, O., Harada, K., Michaels, A.F., Van Der Loeff'o, M.R., Sarin, M., Steinberg, D.K., Trull, T., 2007. An assessment of the use of sediment traps for estimating upper ocean particle fluxes. J. Mar. Res. 65, 345–416.

Cacchione, D.A., Drake, D.E., 1986. Nepheloid layers and internal waves over continental shelves and slopes. Geo-Mar. Lett. 6, 147–152.

Carmack, E.C., Kulikov, E.A., 1998. Wind-forced upwelling and internal Kelvin wave generation in Mackenzie Canyon, Beaufort Sea. J. Geophys. Res.-Oceans 103, 18447–18458.

Carmack, E.C., Chapman, D.C., 2003. Wind-driven shelf/basin exchange on an Arctic shelf: the joint roles of ice cover extent and shelf-break bathymetry. Geophys. Res. Lett. 30, 1778, http://dx.doi.org/10.1029/2003GL017526.

Conley, D.J., 1998. An interlaboratory comparison for the measurement of biogenic silica in sediments. Mar. Chem. 63, 39–48.

Darby, D.A., Ortiz, J., Polyak, L., Lund, S., Jakobsson, M., Woodgate, R.A., 2009. The role of currents and sea ice in both slowly deposited central Arctic and rapidly deposited Chukchi–Alaskan margin sediments. Global Planet. Change 68, 56–70, http://dx.doi.org/10.1016/j.gloplacha.2009.02.007.

Eicken, H., Gradinger, R., Gaylord, A., Mahoney, A., Rigor, I., Melling, H., 2005. Sediment transport by sea ice in the Chukchi and Beaufort Seas: increasing importance due to changing ice conditions? Deep-Sea Res. Part II 52, 3281–3302, http://dx.doi.org/10.1016/j.dsr2.2005.10.006.

Fahl, K., Nöthig, E.-M., 2007. Lithogenic and biogenic particle fluxes on the Lomonosov Ridge (central Arctic Ocean) and their relevance for sediment accumulation: vertical vs. lateral transport. Deep-Sea Res. Part I 54, 1256–1272, http://dx.doi.org/10.1016/j.dsr.2007.04.014.

Forest, A., Sampei, M., Hattori, H., Makabe, R., Sasaki, H., Fukuchi, M., Wassmann, P., Fortier, L., 2007. Particulate organic carbon fluxes on the slope of the Mackenzie Shelf (Beaufort Sea): physical and biological forcing of shelf-basin exchanges. J. Mar. Sys. 68, 39–54.

Forest, A., Sampei, M., Rail, M.E., Gratton, Y., Fortier, L., 2008. Winter pulses of Pacific-origin water and resuspension events along the Canadian Beaufort slope revealed by a bottom-moored observatory, Oceans 2008, 10747934. University of Laval, Quebec City, QC, Canadahttp://dx.doi.org/10.1109/OCEANS.2008.5152010 1–8.

Giles, K.A., Laxon, S.W., Ridout, A.L., Wingham, D.J., Bacon, S., 2012. Western Arctic Ocean freshwater storage increased by wind-driven spin-up of the Beaufort Gyre. Nat. Geosci. 5, 194–197, http://dx.doi.org/10.1134/S0001433812010136.

Grantz, A., Phillips, R.L., Mullen, M.W., Starratt, S.W., Jones, G.A., Naidu, A.S., Finney, B.P., 1996. Character, paleoenvironment, rate of accumulation, and evidence for seismic triggering of Holocene turbidites, Canada Abyssal Plain, Arctic Ocean. Mar. Geol. 133, 51–73, http://dx.doi.org/10.1016/0025-3227(96)00015-1.

Hill, P.R., Blasco, S.M., Harper, J.R., Fissel, D.B., 1991. Sedimentation on the Canadian Beaufort Shelf. Cont. Shelf Res. 11, 821–842.

Honjo, S., Doherty, K.W., 1988. Large aperture time-series sediment traps: design objectives, construction and application. Deep-Sea Res. 35, 133–149.

Honjo, S., Manganini, S.J., Krishfield, R.A., Francois, R., 2008. Particulate organic carbon fluxes to the ocean interior and factors controlling the biological pump: a synthesis of global sediment trap programs since 1983. Prog. Oceanogr. 76, 217–285.

Honjo, S., Krishfield, R.A., Eglinton, T.I., Manganini, S.J., Kemp, J.N., Doherty, K., Hwang, J., Mckee, T.K., Takizawa, T., 2010. Biological pump processes in the cryopelagic and hemipelagic Arctic Ocean: Canada Basin and Chukchi Rise. Prog. Oceanogr. 85, 137–170, http://dx.doi.org/10.1016/j.pocean.2010.02.009.

Hwang, J., Eglinton, T.I., Krishfield, R.A., Manganini, S.J., Honjo, S., 2008. Lateral organic carbon supply to the deep Canada Basin. Geophys. Res. Lett. 35, L11607, http://dx.doi.org/10.1029/2008GL034271.

Hwang, J., Druffel, E.R.M., Eglinton, T.I., 2010. Widespread influence of resuspended sediments on oceanic particulate organic carbon: insights from radiocarbon and aluminum contents in sinking particles. Global Biogeoch. Cycles 24, GB4016, http://dx.doi.org/10.1029/2010GB003802.

Kadko, D., Pickart, R.S., Mathis, J., 2008. Age characteristics of a shelf-break eddy in the western Arctic and implications for shelf-basin exchange. J. Geophys. Res. C: Oceans 113, C02018, http://dx.doi.org/10.1029/2007JC004429.

Krishfield, R., Plueddemann, A.J., Honjo, S., 2002. Eddys in the Arctic Ocean from IOEB ADCP data. Woods Hole Oceanog. Inst. Tech Rept. WHOI-2002-09. 145.

Kulikov, E.A., Carmack, E.C., Macdonald, R.W., 1998. Flow variability at the continental shelf break of the Mackenzie Shelf in the Beaufort Sea. J. Geophys. Res.-Oceans 103, 12725–12741.

Kulikov, E.A., Rabinovich, A.B., Carmack, E.C., 2004. Barotropic and baroclinic tidal currents on the Mackenzie shelf break in the southeastern Beaufort Sea. J. Geophys. Res. C: Oceans 109, C05020, http://dx.doi.org/10.1029/2003JC001986.

Lalande, C., Bã©Langer, S., Fortier, L., 2009. Impact of a decreasing sea ice cover on the vertical export of particulate organic carbon in the northern Laptev Sea, Siberian Arctic Ocean. Geophys. Res. Lett. 36 , http://dx.doi.org/10.1029/2009GL040570.

Macdonald, R.W., Wong, C.S., 1987. The distribution of nutrients in the southeastern Beaufort Sea—implications for water circulation and primary production. J. Geophys. Res.-Oceans 92, 2939–2952.

Macdonald, R.W., Paton, D.W., Carmack, E.C., Omstedt, A., 1995. The freshwater budget and under-ice spreading of Mackenzie River water in the Canadian Beaufort Sea based on salinity and 18O/16O measurements in water and ice. J. Geophys. Res. 100, 895–919.

Macdonald, R.W., Carmack, E.C., Mclaughlin, F.A., Falkner, K.K., Swift, J.H., 1999. Connections among ice, runoff and atmospheric forcing in the Beaufort Gyre. Geophys. Res. Lett. 26, 2223–2226.

Manson, G.K., Solomon, S.M., 2007. Past and future forcing of Beaufort Sea coastal change. Atmos. Ocean 45, 107–122.

Mathis, J.T., Pickart, R.S., Hansell, D.A., Kadko, D., Bates, N.R., 2007. Eddy transport of organic carbon and nutrients from the Chukchi Shelf: impact on the upper halocline of the western Arctic Ocean. J. Geophys. Res. C: Oceans 112, C05011, http://dx.doi.org/10.1029/2006JC003899.

McGillicuddy, D.J., Anderson, L.A., Bates, N.R., Bibby, T., Buesseler, K.O., Carlson, C.A., Davis, C.S., Ewart, C., Falkowski, P.G., Goldthwait, S.A., Hansell, D.A., Jenkins, W.J., Johnson, R., Kosnyrev, V.K., Ledwell, J.R., Li, Q.P., Siegel, D.A., Steinberg, D.K., 2007. Eddy/wind interactions stimulate extraordinary mid-ocean plankton blooms. Science 316, 1021–1026.

Mizobata, K., Saitoh, S.I., Shiomoto, A., Miyamura, T., Shiga, N., Imai, K., Toratani, M., Kajiwara, Y., Sasaoka, K., 2002. Bering Sea cyclonic and anticyclonic eddies

observed during summer 2000 and 2001. Prog. Oceanogr. 55, 65–75, http://dx.doi.org/10.1016/S0079-6611(02)00070-8.
Morison, J., Kwok, R., Peralta-Ferriz, C., Alkire, M., Rigor, I., Andersen, R., Steele, M., 2012. Changing Arctic Ocean freshwater pathways. Nature 481, 66–70, http://dx.doi.org/10.1038/nature10705.
Mortlock, R.A., Froelich, P.N., 1989. A simple method for the rapid determination of biogenic opal in pelagic marine sediments. Deep Sea Res. 36, 1415–1426.
Mulligan, R.P., Perrie, W., Solomon, S., 2010. Dynamics of the Mackenzie River plume on the inner Beaufort shelf during an open water period in summer. Estuar. Coast. Shelf Sci. 89, 214–220, http://dx.doi.org/10.1016/j.ecss.2010.06.010.
Nikolopoulos, A., Pickart, R.S., Fratantoni, P.S., Shimada, K., Torres, D.J., Jones, E.P., 2009. The western Arctic boundary current at 152 degrees W: structure, variability, and transport. Deep-Sea Res. Part II 56, 1164–1181, http://dx.doi.org/10.1016/j.dsr2.2008.10.014.
O'Brien, M.C., Macdonald, R.W., Melling, H., Iseki, K., 2006. Particle fluxes and geochemistry on the Canadian Beaufort Shelf: implications for sediment transport and deposition. Cont. Shelf Res. 26, 41–81, http://dx.doi.org/10.1016/j.csr.2005.09.007.
O'Brien, M.C., 2009, Physical Processes and Biogeochemistry of Particle Fluxes over the Beaufort Slope and in Canada Basin. Master of Science Thesis. University of Victoria British Columbia, Canada. 〈https://dspace.library.uvic.ca:8443/bitstream/1828/1669/10/OBrien_2009_Final.pdf〉. [Note: Current speeds for the A01 Canada Basin moorings in O'Brien (2009) have been reprocessed to correct an error in the original processing—the corrected current speeds are reported in this article.].
O'Brien, M.C., Melling, H., Pedersen, T.F., Macdonald, R.W., 2011. The role of eddies and energetic ocean phenomena in the transport of sediment from shelf to basin in the Arctic. J. Geophys. Res.-Oceans 116, C08001, http://dx.doi.org/10.1029/2010JC006890.
Parsons, T.R., Maita, Y., Lalli, C.M., 1984. A Manual of Chemical and Biological Methods for Seawater Analysis. Pergamon Press, Oxford, pp. 173.
Pelletier, B.R., 1984. Marine Science Atlas of the Beaufort Sea: Sediments. Miscellaneous Report 38; Geological Survey of Canada. 27 pp.
Pickart, R.S., 2004. Shelfbreak circulation in the Alaskan Beaufort Sea: mean structure and variability. J. Geophys. Res. C: Oceans 109, C04024, doi:04010.01029/02003JC001912.
Plueddemann, A.J., Krishfield, R., Takizawa, T., Hatakeyama, K., Honjo, S., 1998. Upper ocean velocities in the Beaufort Gyre. Geophys.Res. Lett. 25, 183–186.
Proshutinsky, A.Y., Johnson, M.A., 1997. Two circulation regimes of the wind driven Arctic Ocean. J. Geophys. Res.-Oceans 102, 12493–12514.
Proshutinsky, A.Y., Polyakov, I.V., Johnson, M.A., 1999. Climate states and variability of Arctic ice and water dynamics during 1946–1997. Polar Res. 18, 135–142.
Proshutinsky, A., Bourke, R.H., Mclaughlin, F.A., 2002. The role of the Beaufort Gyre in Arctic climate variability: seasonal to decadal climate scales. Geophys. Res. Lett. 29, 2100, doi:2110.1029/2002GL015847.
Rachold, V., Eicken, H., Gordeev, V.V., Grigoriev, M.N., Hubberten, H.-W., Lisitzin, A.P., Shevchenko, V.P., Schirrmeister, L., 2004. Modern terrigenous organic input into the Arctic Ocean. In: Stein, R., Macdonald, R.W. (Eds.), The Arctic Ocean Organic Carbon Cycle: Present and Past, 2003. Springer, Berlin-Heidelberg-New York, pp. 33–55, Chapter 2.
Ragueneau, O., Treguer, P., 1994. Determination of biogenic silica in coastal waters—applicability and limits of the alkaline digestion method. Mar. Chem. 45, 43–51.
Ragueneau, O., Savoye, N., Del Amo, Y., Cotten, J., Tardiveau, B., Leynaert, A., 2005. A new method for the measurement of biogenic silica in suspended matter of coastal waters: using Si:Al ratios to correct for the mineral interference. Cont. Shelf Res. 25, 697–710, http://dx.doi.org/10.1016/j.csr.2004.09.017.
Spall, M.A., Pickart, R.S., Fratantoni, P.S., Plueddemann, A.J., 2007. Western Arctic shelfbreak eddies: formation and transport. J. Phys. Oceanogr. 38, 1644–1668.
Stein, R., Macdonald, R.W., 2004. In: Stein, R., Macdonald, R.W. (Eds.), The organic carbon cycle in the Arctic Ocean. Springer, pp. 363.
Williams, W.J., Carmack, E.C., Shimada, K., Melling, H., Aagaard, K., Macdonald, R.W., Ingram, R.G., 2006. Joint effects of wind and ice motion in forcing upwelling in Mackenzie Trough, Beaufort Sea. Cont. Shelf Res. 26, 2352–2366, http://dx.doi.org/10.1016/j.csr.2006.06.012.
Williams, W.J., Melling, H., Carmack, E.C., Ingram, R.G., 2008. Kugmallit Valley as a conduit for cross-shelf exchange on the Mackenzie Shelf in the Beaufort Sea. J. Geophys. Res. C: Oceans 113, C02007, doi:10.01029/02006JC003591.
Yang, J.Y., 2009. Seasonal and interannual variability of downwelling in the Beaufort Sea. J. Geophys. Res.-Oceans 114, C00A14, http://dx.doi.org/10.1029/2008JC005084.